

## Deep Ancestral Introgression Shapes Evolutionary History of Dragonflies and Damselflies

ANTON SUVOROV<sup>1,\*</sup>, CELINE SCORNAVACCA<sup>2,†</sup>, M. STANLEY FUJIMOTO<sup>3</sup>, PAUL BODILY<sup>4</sup>, MARK CLEMENT<sup>3</sup>, KEITH A. CRANDALL<sup>5</sup>, MICHAEL F. WHITING<sup>6,7</sup>, DANIEL R. SCHRIDER<sup>1,†</sup>, AND SETH M. BYBEE<sup>6,7,†</sup>

<sup>1</sup>Department of Genetics, University of North Carolina at Chapel Hill, Chapel Hill, NC 27599, USA; <sup>2</sup>Institut des Sciences de l'Evolution Université de Montpellier, CNRS, IRD, EPHE CC 064, Place Eugène Bataillon, 34095 Montpellier Cedex 05, France; <sup>3</sup>Department of Computer Science, Brigham Young University, Provo, UT 84602, USA; <sup>4</sup>Department of Computer Science, Idaho State University, Pocatello, ID 83209, USA; <sup>5</sup>Computational Biology Institute, Department of Biostatistics and Bioinformatics, Milken Institute School of Public Health, George Washington University, Washington, DC 20052, USA; <sup>6</sup>Department of Biology, Brigham Young University, Provo, UT 84602, USA; and <sup>7</sup>M.L. Bean Museum, Brigham Young University, Provo, UT 84602, USA  
\*Correspondence to be sent to: Department of Genetics, University of North Carolina at Chapel Hill, 120 Mason Farm Road, UNC-Chapel Hill, Chapel Hill, NC 27599-7264, USA

E-mail: [anton.suvorov@med.unc.edu](mailto:anton.suvorov@med.unc.edu)

<sup>†</sup>Celine Scornavacca, Daniel R. Schrider, and Seth M. Bybee contributed equally to this article.

Received 21 March 2021; reviews returned 20 July 2021; accepted 26 July 2021

Associate Editor: Michael Matschiner

**Abstract.**—Introgression is an important biological process affecting at least 10% of the extant species in the animal kingdom. Introgression significantly impacts inference of phylogenetic species relationships where a strictly binary tree model cannot adequately explain reticulate net-like species relationships. Here, we use phylogenomic approaches to understand patterns of introgression along the evolutionary history of a unique, nonmodel insect system: dragonflies and damselflies (Odonata). We demonstrate that introgression is a pervasive evolutionary force across various taxonomic levels within Odonata. In particular, we show that the morphologically “intermediate” species of Anisozygoptera (one of the three primary suborders within Odonata besides Zygoptera and Anisoptera), which retain phenotypic characteristics of the other two suborders, experienced high levels of introgression likely coming from zygopteran genomes. Additionally, we find evidence for multiple cases of deep inter-superfamilial ancestral introgression. [Gene flow; Odonata; phylogenomics; reticulate evolution.]

In recent years, numerous studies have showed that multiple parts of the Tree of Life did not evolve according to a strictly bifurcating phylogeny (Hallstrom and Janke 2010; Mallet et al. 2016). Instead, many organisms experience reticulate network-like evolution that is caused by an exchange of interspecific genetic information via various biological processes. In particular, lateral gene transfer, incomplete lineage sorting (ILS), and introgression can result in gene trees that are discordant with the species tree (Maddison 1997; Posada and Crandall 2001; Degnan and Rosenberg 2009). Lateral transfer and introgression both involve gene flow following speciation, thereby producing “reticulate” phylogenies. ILS, on the other hand, occurs when lineages fail to coalesce within their ancestral population. Since this process does not involve any postspeciation gene flow, it does not contribute to reticulate evolution, even though it often results in discordant gene trees. Phylogenetic species-gene tree incongruence observed in empirical data can provide insight into underlying biological factors that shape the evolutionary trajectories of a set of taxa. The major source of reticulate evolution for eukaryotes is introgression where it affects approximately 25% of flowering plant and 10% of animal species (Mallet 2005; Mallet et al. 2016). Introgressed alleles can be fitness-neutral, deleterious (Petr et al. 2019), or adaptive (Norris et al. 2015; Oziolor et al. 2019). For example, adaptive introgression has been shown to provide an evolutionary rescue from polluted habitats in gulf killifish (*Fundulus grandis*; Oziolor et al. 2019), yielded mimicry adaptations among

*Heliconius* butterflies (Heliconius Genome Consortium 2012) and archaic introgression has facilitated adaptive evolution of altitude tolerance (Huerta-Sanchez et al. 2014), immunity and metabolism in modern humans (Gouy and Excoffier 2020). Additionally, hybridization and introgression are important and often overlooked mechanisms of invasive species establishment and spread (Perry et al. 2002).

Odonata, the insect order that contains dragonflies and damselflies, lacks a strongly supported backbone tree to clearly resolve higher-level phylogenetic relationships (Dijkstra, Kalkman et al. 2014; Carle et al. 2015). Current evidence places odonates together with Ephemeroptera (mayflies) as the living representatives of the most ancient insect lineages to have evolved wings and active flight (Thomas et al. 2013). Odonates possess unique anatomical and morphological features such as a specialized body form, specialized wing venation, a distinctive form of muscle attachment to the wing base (Busse et al. 2013) allowing for direct flight and accessory (secondary) male genitalia that support certain unique behaviors (e.g., sperm competition). They are among the most adept flyers of all animals and are exclusively carnivorous insects relying primarily on vision to capture prey (Chauhan et al. 2014; Suvorov et al. 2017). During their immature stage, they are fully aquatic and spend much of their adult life in flight. Biogeographically, odonates exhibit species ranges varying from worldwide dispersal (Troast et al. 2016) to island-endemic. Odonates also play crucial ecological roles in local freshwater communities, being a top invertebrate predator as both adults and immatures

(Dijkstra, Monaghan et al. 2014). Due to this combination of characteristics, odonates are quickly becoming model organisms to study specific questions in ecology, physiology, and evolution (Cordoba-Aguilar 2008; Bybee et al. 2016). However, the extent of introgression at the genomic scale within Odonata remains largely unknown.

In various biological systems, the empirical evidence shows that hybridization can potentially lead to intermediate phenotypes (Runemark et al. 2019) observed at molecular level (e.g. semidominant expression in interspecific hybrids; Landry et al. 2005) as well as organismal morphology (e.g. Lemmon and Lemmon 2010; Rothfels et al. 2015; Káldy et al. 2020). The Anisozygoptera suborder, which contains only three extant species, retains traits shared with both dragonflies and damselflies (hence its taxonomic name), ranging from morphology and anatomical structures (Busse et al. 2015) to behavior and flight biomechanics (Ruppell and Hilfert 1993). These characteristics could suggest either a hybrid origin of this suborder or substantial introgression at loci governing key morphological and behavioral traits shortly after the suborder's formation. The potential introgression scenario for Anisozygoptera is yet to be formally tested using genome-wide data. Two early attempts to tackle introgression/hybridization patterns within Odonata were undertaken in (Monetti et al. 2002; Sánchez-Guillén et al. 2005). The studies showed that two closely related species of damselflies, *Ischnura graellsii* and *Ischnura elegans*, can hybridize under laboratory conditions and that genital morphology of male hybrids shares features with putative hybrids from *I. graellsii* to *I. elegans* natural allopatric populations (Monetti et al. 2002). The existence of abundant hybridization and introgression in natural populations of *I. graellsii* and *I. elegans* has received further support from an analysis of microsatellite data (Sanchez-Guillen et al. 2011). Putative hybridization events have also been identified in a pair of calopterygoid damselfly species, *Mnais costalis* and *Mnais pruinosa* based on the analyses of two molecular loci (mtDNA and nucDNA; Hayashi et al. 2005), and between *Calopteryx virgo* and *Calopteryx splendens* using 16S ribosomal DNA and 40 random amplified polymorphic DNA markers (Tynkynen et al. 2008). A more recent study identified an interspecific hybridization between two cordulegasterid dragonfly species, *Cordulegaster boltonii* and *Cordulegaster trinacriae* using two molecular markers (mtDNA and nucDNA) and geometric morphometrics (Solano et al. 2018).

Here, we present a comprehensive analysis of transcriptomic data from 83 odonate species. First, we reconstruct a robust phylogenetic backbone using up to 4341 genetic loci for the order and discuss its evolutionary history spanning from the Carboniferous period (~360 Ma) to present day. Furthermore, in light of the “intermediate” phenotypic nature of Anisozygoptera, we investigate phylogenetic signatures of introgression within Odonata. Most notably, we

identify a strong signal of deep introgression in the Anisozygoptera suborder, species of which possess traits of both main suborders, Anisoptera and Zygoptera. Although the strongest signatures of introgression are found in Anisozygoptera, we find evidence that introgression was pervasive in Odonata throughout its entire evolutionary history.

## MATERIALS AND METHODS

### *Taxon Sampling and RNA-seq*

In this study, we used 85 distinct species (83 ingroup and 2 outgroup taxa). Thirty-five RNA-seq libraries were obtained from NCBI (Supplementary Table S1 available on Dryad at <https://doi.org/10.5061/dryad.j3tx95xdp>). The remaining 58 libraries were sequenced in the Bybee Lab (some species have several RNA-seq libraries; Supplementary Table S1 available on Dryad). Total RNA was extracted for each taxon from eye tissue using NucleoSpin columns (Clontech) and reverse-transcribed into cDNA libraries using the Illumina TruSeq RNA v2 sample preparation kit that both generates and amplifies full-length cDNAs. Prepped mRNA libraries with insert size of ~200 bp were multiplexed and sequenced on an Illumina HiSeq 2000 producing paired-end reads with average length of 275 bp by the Microarray and Genomic Analysis Core Facility at the Huntsman Cancer Institute at the University of Utah, Salt Lake City, UT, USA. Quality scores, tissue type, and other information about RNA-seq libraries are summarized in Supplementary Table S1 available on Dryad and NCBI BioProject PRJNA641626.

### *Transcriptome Assembly and CDS Prediction*

RNA-seq libraries were trimmed and de novo assembled using Trinity (Grabherr et al. 2011; Haas et al. 2013) with default parameters. Then only the longest isoform was selected from each gene for downstream analyses using the Trinity utility script. In order to identify potentially coding regions within the transcriptomes, we used TransDecoder with default parameters specifying to predict only the single best ORF. Each predicted proteome was screened for contamination using DIMOND BLASTP (Buchfink et al. 2015) with an *E*-value cutoff of  $10^{-10}$  against custom protein database. Nonarthropod hits were discarded from proteomes (amino acid, AA sequences) and corresponding CDSs. To mitigate redundancy in proteomes and CDSs, we used CD-HIT (Fu et al. 2012) with the identity threshold of 0.99. Such a conservative threshold was used to prevent exclusion of true paralogous sequences; thus, reducing possible false-positive detection of 1:1 orthologs during homology searches.

### *Homology Assessment*

In the present study, three types of homologous loci (gene clusters), namely conserved single-copy orthologs (CO), all single-copy orthologs (AO), and

paralogy-parsed orthologs (PO) identified by BUSCO v1.22 (Simao et al. 2015), OrthoMCL (Li et al. 2003), and (Yang and Smith, 2014) pipelines, respectively, were used in phylogenetic inference.

BUSCO arthropod Hidden Markov Model Profiles of 2675 single-copy orthologs were used to find significant COs matches within CDS data sets by HMMER's *hmmsearch* v3 (Eddy 2011) with group-specific expected bit-score cutoffs. BUSCO classifies loci into complete [duplicated] and fragmented. Thus, only complete single-copy loci were extracted from CDS data sets and corresponding AA sequences for further phylogenetic analyses. Since loci were identified as true orthologs if they score above expected bit-score, and complete if their lengths lie within ~95% of BUSCO group mean length, many partial erroneously assembled sequences were filtered out.

OrthoMCL v2.0.9 (Li et al. 2003) was used to compute AOs in all species using predicted AA sequences by TransDecoder. AA sequences were used in an all-vs-all BLASTP with an *E*-value cutoff of  $10^{-10}$  to find putative orthologs and paralogs. The Markov Cluster algorithm (MCL) inflation point parameter was set to 2. Only 1:1 orthologs were used in further analyses. In order to exclude false-positive homology clusters identified by OrthoMCL, we applied machine learning filtering procedure (Fujimoto et al. 2016) implemented in OGCleaner software v1.0 (Fujimoto et al. 2017) using a metaclassifier with logistic regression.

Finally, to identify additional clusters, we used Yang and Smith's tree-based orthology inference pipeline (Yang and Smith 2014) that was specifically designed for nonmodel organisms using transcriptomic data. Yang and Smith's algorithm is capable of parsing paralogous gene families into "orthology" clusters that can be used in phylogenetic analyses. It has been shown that paralogous sequences encompass useful phylogenetic information (Hellmuth et al. 2015). First, the Transdecoder-predicted AA sequences were trimmed using CD-HIT with the identity threshold of 0.995. Then, all-vs-all BLASTP with an *E*-value cutoff of  $10^{-5}$  search was implemented. The raw BLASTP output was filtered by a hit fraction of 0.4. Then, MCL clustering was performed with an inflation point parameter of 2. Each cluster was aligned using iterative algorithm of PASTA (Mirarab et al. 2015) and then was used to infer a maximum-likelihood (ML) gene tree using IQ TREE v1.5.2 (Nguyen et al. 2015) with an automatic model selection. Tree tips that were longer than relative and absolute cutoffs of 0.4 and 1, respectively, were removed. Mono- and paraphyletic tips that belonged to the same species were masked as well. To increase quality of homology clusters realignment, tree inference, and tip masking steps were iterated with more stringent relative and absolute masking cutoffs of 0.2 and 0.5, respectively. Finally, POs (AA sequences and corresponding CDSs) were extracted by rooted ingroups (RI) procedure using *Ephemera danica* as an outgroup (for details see Yang and Smith 2014).

#### Cluster Alignment, Trimming, and Supermatrix Assembly

For most of the analyses, only clusters with  $\geq 42$  (~50%) species present were retained. In total, we obtained five cluster types, namely DNA (CDS) and AA COs, AA AOs and DNA and AA POs. Each cluster was aligned using PASTA (Mirarab et al. 2015) for the DNA and AA alignments and PRANK v150803 (Loytynoja and Goldman 2008; Loytynoja 2014) for the codon alignments and alignments where either 1st and 2nd or 3rd codon positions were removed. In order to reduce the amount of randomly aligned regions, we implemented ALIScore v2.0 (Misof and Misof 2009) trimming procedure (for PASTA alignments) followed by masking any site with  $\geq 42$  gap characters (for both PASTA and PRANK alignments). Also, since fragmentary data may have a negative effect on accuracy of gene and hence species tree inference (Wickett et al. 2014), sequence fragments with  $>50\%$  gap characters were removed from clusters that were used to estimate trees with ASTRAL v4.10.12 (Mirarab et al. 2014). For each of the cluster type, we assembled supermatrices from trimmed gene alignments. Additionally, completely untrimmed supermatrices were generated from DNA and AA COs with  $\geq 5$  species present.

#### Phylogenetic Tree Reconstruction

Four different in spirit tree-building methods (ML:IQTREE, Bayesian:ExaBayes, Supertree:ASTRAL, Alignment-Free [AF]: Co-phylog) were used to infer odonate phylogenetic relationships using different input data types (untrimmed and trimmed supermatrices, codon supermatrices, codon supermatrices with 1st and 2nd or 3rd positions removed, gene trees, and assembled transcriptomes). In total, we performed 48 phylogenetic analyses and compared topologies to identify stable and conflicting relationships (Supplementary Table S2 available on Dryad).

We inferred phylogenetic ML trees from each supermatrix using IQTREE implementing two partitioning schemes: single partition and those identified by PartitionFinder v2.0 (three GTR models for DNA and a large array of protein models for AA; Lanfear et al. 2017) with relaxed hierarchical clustering option (Lanfear et al. 2014). In the first case, IQTREE was run allowing model selection and assessing nodal support with 1000 ultrafast bootstrap (UFBoot; (Minh et al. 2013)) replicates. In the second case, IQTREE was run with a given PartitionFinder partition model applying gene and site resampling to minimize false positives (Gadagkar et al. 2005) for 1000 UFBoot replicates.

For Bayesian analyses implemented in ExaBayes (Aberer et al. 2014), we used highly trimmed (retaining sites only with occupancy of  $\leq 5$  gap characters) and original DNA and AA CO supermatrices assuming a single partition. We initiated four independent runs with four Markov Chain Monte Carlo (MCMC) coupled chains sampling every 500th iteration. Due to high computational demands of the procedure, only the GTR

and JTT substitution model priors were applied to DNA and AA CO supermatrices, respectively, with the default topology, rate heterogeneity, and branch lengths priors. However, all supported protein substitution models as a prior were specified for the trimmed AA CO supermatrix. For convergence criteria, an average standard deviation of split frequencies (ASDSF; Lakner et al. 2008), a potential scale reduction factor (PSRF; Brooks and Gelman 1998), and an effective sample size (ESS; Lanfear et al. 2017) were utilized. Values of 0% <ASDSF <1% and 1% <ASDSF <5% indicate excellent and acceptable convergence, respectively; ESS >100 and PSRF ~1 represent good convergence (see ExaBayes manual; Aberer et al. 2014).

ASTRAL analyses were conducted using two input types: 1) gene trees obtained by IQTREE allowing model selection for fully trimmed DNA and AA clusters and 2) gene trees obtained from the alignment-tree coestimation process in PASTA. Nodal support was assessed by local posterior probabilities (Sayyari and Mirarab 2016). In addition to standard phylogenetic inferential approaches, we applied an AF species tree estimation algorithm using Co-phylog (Yi and Jin 2013). Raw Transdecoder CDS outputs were used in this analysis using k-mer size of 9 as the half context length required for Co-phylog. Bootstrap replicate trees were obtained by running Co-Phylog with the same parameter settings on each subsampled with replacement CDS Transdecoder libraries and were used to assess nodal support.

#### Assessment of Phylogenetic Support via Quartet Sampling

As an additional phylogenetic support, we implemented quartet sampling (QS) approach (Pease et al. 2018). Briefly, this method provides three scores for internal nodes: 1) the quartet concordance (QC) score gives an estimate of how sampled quartet topologies agree with the putative species tree; 2) quartet differential (QD) estimates frequency skewness of the discordant quartet topologies, which can be indicative of introgression if a skewed frequency is observed; and 3) quartet informativeness (QI) quantifies how informative sampled quartets are by comparing likelihood scores of alternative quartet topologies. Finally, QS provides a quartet fidelity score for terminal nodes that measures a taxon “rogueness.” We performed QS analysis with all 48 putative species phylogenies using the SuperMatrix\_50BUSCO\_dna\_pasta\_ali\_trim supermatrix, specifying the IQTREE engine for quartet likelihood calculations with 100 replicates (i.e., number of quartet draws per focal branch).

#### Fossil Dating

A Bayesian algorithm of MCMCTree v4.9h (Yang 2007) with approximate likelihood computation was implemented to estimate divergence times within Odonata using 20 crown node fossil constraints with

corresponding prior distributions (Supplementary Table S3 available on Dryad). First, we estimated branch lengths by ML and then the gradient and Hessian matrix around these ML estimates in MCMCTree using SuperMatrix\_50BUSCO\_dna\_pasta\_ali\_trim supermatrix. Second, we used these gradient and Hessian matrices to construct an approximate likelihood function by Taylor expansion (Dos Reis and Yang 2011) and perform fossil calibration in MCMC framework under the uncorrelated clock model. For this step, we specified GTR+ $\Gamma$  substitution model with four gamma categories, along with birth, death, and sampling parameters of 1, 0.5, and 0.01, respectively. To ensure convergence, the analysis was run independently five times for  $6 \times 10^7$  generations, logging every 1000th generation and then removing 50% as a burn-in. Convergence (ESS >200) of the MCMC chains was verified using Tracer v1.71 (Rambaut et al. 2018). Visualization of the calibrated tree was performed in R using the MCMCTreeR package (Puttick 2019).

#### Analyses of Introgression

In order to address the scope of possible reticulate evolution across odonate phylogeny, we used various methods of introgression detection such as HyDe/D (Blischak et al. 2018),  $D_{FOIL}$  (Pease and Hahn 2015),  $\chi^2$  goodness-of-fit test, branch length test (BLT), QuIBL (Edelman et al. 2019), and PhyloNet (Than et al. 2008; Wen et al. 2018). Furthermore, we used the methodological consensus of HyDe/D,  $D_{FOIL}$ ,  $\chi^2$  goodness-of-fit test, and BLT approaches to provide more conservative inferences of introgression across the order (see Discussion section). Specifically, we compared sets of unique introgressing species pairs that were identified by each of the aforementioned methods. The significance of overlap among the signals from these different methods was then assessed using an exact test of multiset interactions (Wang et al. 2015).

The HyDe framework allows detection of hybridization events which relies on quantification of phylogenetic site patterns. HyDe estimates whether a putative hybrid population (or taxon) H is sister to either population P1 with probability  $\gamma$  or to P2 with probability  $1-\gamma$  in a 4-taxon (quartet) tree ((P1,H,P2),O), where O denotes an outgroup. Then, it conducts a formal statistical test of  $H_0: \gamma = 0$  vs.  $H_1: \gamma > 0$  using Z-test, where  $\gamma = 0$  (=1) is indicative of nonsignificant introgression. We applied HyDe to the concatenated supermatrix SuperMatrix\_50BUSCO\_dna\_pasta\_ali\_trim of 1603 BUSCO genes under default parameters specifying *E. danica* as an outgroup. Under this setup, HyDe evaluates all possible taxa quartets. Since HyDe only allows indication of a single outgroup taxon (i.e. *E. danica*), we excluded all quartets that contained the *Isonychia kiangsinensis* outgroup from the HyDe output. Additionally, we calculated Patterson’s *D* statistic (Patterson et al. 2012) for every quartet from the frequency (*p*) of ABBA-BABA site patterns estimated

by HyDe as  $D = \frac{p_{ABBA} - p_{BABA}}{p_{ABBA} + p_{BABA}}$ . To test significance of  $D$  statistics, we used a  $\chi^2$  test to assess whether the proportions  $p_{ABBA}$  and  $p_{BABA}$  were significantly different. To minimize effect of false-positive cases (type I error) in the output, we first applied a Bonferroni correction to the  $P$ -values derived from  $Z$ - and  $\chi^2$  tests and then filtered the results based on a significance level of 0.05 and  $10^{-6}$  for  $D$  and  $\gamma$ , respectively. Additionally, we excluded all quartets that did not match the species topology. Furthermore, we ran HyDe on SuperMatrix\_50BUSCO\_dna\_prank\_trim excluding 3rd codon position to investigate a potential impact of the saturation effect on introgression inference.

$D_{FOIL}$  is an alternative site pattern-based approach that detects introgression using symmetric 5-taxon (quintet) trees, i.e.  $((P1,P2),(P3,P4)),O$ .  $D_{FOIL}$  represents a collection of statistics for quintet trees that are similar in spirit to the Patterson's  $D$  statistic; if considered simultaneously, these statistics provide a powerful approach to identify introgression including ancestral as well as donor and recipient taxa (i.e. introgression directionality). Moreover,  $D_{FOIL}$  exhibits exceptionally low false-positive rates (Pease and Hahn 2015). Since the number of possible quintet topologies for a phylogeny of 85 taxa is  $>32 \times 10^6$ , for analysis we extracted them only for every odonate suborder individually using custom R scripts. Note that for Anisozygoptera, we only considered quintets that can be formed between Anisozygoptera, Anisoptera, and Zygoptera taxonomic groups. As the number of Anisozygoptera quintets is highly disproportional (34,619 out of all 72,971 tested Odonata quintets), for downstream analyses, we randomly selected 4000 Anisozygoptera quintets which approximately matches the number of quintets for an individual species. Analogously to HyDe, we applied  $D_{FOIL}$  to the concatenated supermatrix SuperMatrix\_50BUSCO\_dna\_pasta\_ali\_trim of 1603 BUSCO genes under default parameters specifying *E. danica* as an outgroup. Also, since  $D_{FOIL}$  requires that every quintet has a symmetric topology, we considered only those quintets within our phylogeny that met this criterion (Fig. 1). Additionally,  $D_{FOIL}$  requires that the divergence time of P3 and P4 precedes divergence of P1 and P2, i.e.  $T_2 > T_1$ , thus we filtered out quintets that violated this assumption using divergence times from our fossil calibrated phylogeny. In order to correct the  $P$ -values resulted from  $D_{FOIL}$  analysis for multiple testing, we applied the Benjamini–Hochberg procedure at a false discovery rate (FDR) cutoff of 0.05.

As an alternative test for introgression, we performed a simple yet conservative  $\chi^2$  goodness-of-fit test on the gene count values for each triplet. Specifically, we asked whether one of the two possible discordant gene tree topologies was supported by a greater number of genes than the other discordant topology (i.e. a significant difference between the number of discordant gene trees showing  $((P1,P3),P2)$  vs.  $((P2,P3),P1)$ , where the  $((P1,P2),P3)$  topology corresponds to the species tree).

Under ILS alone, the fractions of genes supporting each discordant topology are expected to be the same, while in the presence of introgression they may differ. We, therefore, used a  $\chi^2$  test to determine if these fractions differed significantly, and we considered triplets where the null hypothesis was rejected to be suggestive of introgression. Because we tested many triplets for introgression, we corrected the  $P$ -values resulted from these  $\chi^2$  tests using the Benjamini–Hochberg procedure and applied an FDR cutoff of 0.05. Second, we used a BLT to identify cases of introgression (Suvorov et al. 2021). This test examines branch lengths to estimate the age of the most recent coalescence event (measured in substitutions per site). Introgression should result in more recent coalescences than expected under the concordant topology with complete lineage sorting, while ILS yields older coalescence events. Importantly, ILS alone is not expected to result in different coalescence times between the two discordant topologies, and this forms the null hypothesis for the BLT. For a given triplet, for each gene tree, we calculated the distance  $d$  (a proxy for the divergence time between sister taxa) by averaging the external branch lengths leading to the two sister taxa under that gene tree topology. We calculated  $d$  for each gene tree and denote values of  $d$  from the first discordant topology  $d_{T1}$  and those from the second discordant topology  $d_{T2}$ . We then compared the distributions of  $d_{T1}$  and  $d_{T2}$  using a Wilcoxon Rank Sum Test. Under ILS alone the expectation is that  $d_{T1} = d_{T2}$ , while in the presence of introgression  $d_{T1} < d_{T2}$  (suggesting introgression consistent with discordant topology  $T_1$ ) or  $d_{T1} > d_{T2}$  (suggesting introgression consistent with discordant topology  $T_2$ ). The BLT is conceptually similar to the D3 test (Hahn and Hibbins 2019), which transforms the values of  $d_{T1}$  and  $d_{T2}$  in a manner similar to the  $D$  statistic for detecting introgression. As with the  $\chi^2$  test, we performed the BLT on all triplets within a clade and used a Benjamini–Hochberg correction with an FDR cutoff of 0.05. We note that both the  $\chi^2$  test and BLT may be conservative in cases where there is introgression between both tested species pairs (i.e. introgression between P1–P3 and P2–P3 for a given species topology  $((P1,P2),P3)$ ) depending on the fraction of affected loci (affects the  $\chi^2$  test) and timing of introgression between each species pair (affects the BLT).

QuIBL is based on the analysis of branch length distributions across gene trees to infer putative introgression patterns. Briefly, under coalescent theory, internal branches of rooted gene trees for a set of 3 taxa (triplet) can be viewed as a mixture of two distributions with the underlying parameters. Each mixture component generates branch lengths corresponding to either ILS or introgression/speciation. Thus, estimated mixing proportions ( $\pi_1$  for ILS and  $\pi_2$  for introgression/speciation;  $\pi_1 + \pi_2 = 1$ ) of those distribution components show what fraction of the gene trees were generated through ILS or non-ILS processes. For a given triplet, QuIBL computes frequency of gene trees that support three alternative

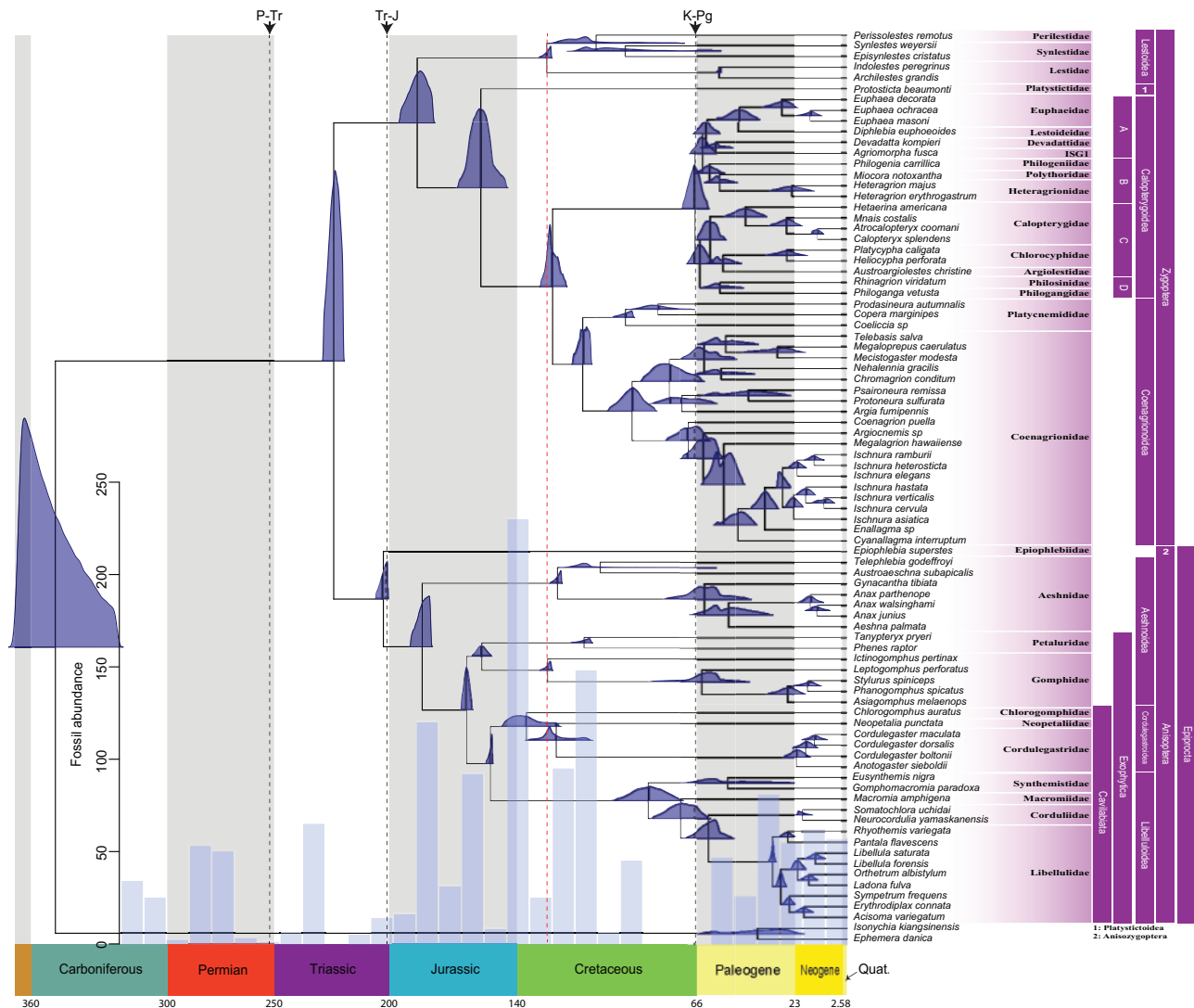


FIGURE 1. Evolutionary history of Odonata. Fossil calibrated ML phylogenetic tree of Odonata using a DNA supermatrix consisting of 1603 BUSCO genes with a total of 2,167,861 aligned sites. The blue densities at each node represent posterior distributions of ages estimated in MCMCTree using 20 fossil calibration points. The red-dashed vertical line indicates the beginning of establishment for major Odonata lineages originating in and spanning the Cretaceous. The histogram (blue bars) represents temporal distribution of fossil Odonata samples. The black-dashed vertical lines mark major extinction events, namely Permian-Triassic (P-Tr, ~251 Ma), Triassic-Jurassic (Tr-J, ~201.3 Ma), and Cretaceous-Paleogene (K-Pg, ~66 Ma)

topologies. Then for every alternative topology, QuIBL estimates mixing proportions along with other relevant parameters via Expectation-Maximization and computes Bayesian Information Criterion (BIC) scores for ILS-only and introgression models. For concordant topologies, elevated values of  $\pi_2$  are expected whereas for discordant ones  $\pi_2$  can vary depending on the severity of ILS/intensity of introgression. In extreme cases when the gene trees were generated exclusively under ILS,  $\pi_2$  will approach zero and the expected gene tree frequency for each alternative topology of a triplet will be approximately 1/3. To identify significant cases of introgression here we used a stringent cutoff of  $\Delta\text{BIC} < -30$  (Edelman et al. 2019). We ran QuIBL on every triplet individually under default parameters

with number of steps (numsteps parameter) is equal to 50 and specifying one of the Ephemeroptera species (*I. kiangsinensis* and *E. danica*) for triplet rooting. For computational efficiency, we extracted triplets only from the Odonata superfamilies in a similar manner as we did for  $D_{\text{FOIL}}$  (see above). For this analysis, we used 1603 ML gene trees estimated from CO orthology clusters. We note that most of the phylogenomic-based introgression detection methods, including approaches used here (namely HyDe,  $D_{\text{FOIL}}$ ,  $\chi^2$  test, BLT, and QuIBL) are not able to infer gene flow between sister lineages (Hibbins and Hahn 2021) as they rely on topological discordance at either the gene or site level, which can only be examined for topologies with more than two taxa.

To identify patterns of reticulate evolution for Anisozygoptera, we estimated phylogenetic networks from the 1603 ML gene trees estimated from CO orthology clusters using pseudolikelihood (InferNetwork\_MPL; Yu and Nakhleh 2015) and likelihood (CalGTProb) approaches implemented in PhyloNet (Than et al. 2008; Wen et al. 2018). For scalability purposes, we subsampled our taxon set to eight Zygoptera species, nine Anisoptera species, and *Epiophlebia superstes*. For all network searches, we explicitly indicated *E. superstes* as a putative hybrid (-h option). For both pseudolikelihood and likelihood analyses, we only selected gene trees that had at least one of the outgroup species (*I. kiangsinensis* and *E. danica*) and at least three ingroup taxa. For pseudolikelihood analysis, we ran PhyloNet allowing a single reticulation event, with the starting tree that corresponds to the species phylogeny (-s option), 100 iterations (-x option), 0.9 bootstrap threshold for gene trees (-b option), and optimization of branch lengths and inheritance probabilities on the inferred networks (-po option). To ensure convergence, the network searches were repeated three times. For the full likelihood estimation, we fixed the topology (equivalent to the species tree topology) and calculated likelihood scores for possible networks with a single reticulation (generated with a custom script) using CalGTProb. Additionally, to assess significance of networks, we used difference of BIC scores ( $\Delta$ BIC) derived from network without reticulation (i.e. tree) and a network with a reticulation (Supplementary Table S4 available on Dryad).

#### Dimensionality Reduction and Visualization

To uncover and visualize complex relationships between site pattern frequencies and Patterson's D statistic and HyDe  $\gamma$  parameter, we implemented a dimensionality reduction technique t-distributed stochastic neighbor embedding (tSNE; van der Maaten and Hinton 2008) under default parameters in R. Specifically, we estimated tSNE maps from counts of 15 quartet site patterns calculated by HyDe ("AAAA," "AAAB," "AABA," "AABB," "AABC," "ABAA," "ABAB," "ABAC," "ABBA," "BAAA," "ABBC," "CABC," "BACA," "BCAA," and "ABCD").

## RESULTS

### Phylogenetic Inference

We compiled transcriptomic data for 83 odonate species including 49 new transcriptomes sequenced for this study (Supplementary Table S1 available on Dryad). To assess effects of various steps of our phylogenetic pipeline on species tree inference, we examined different methods of sequence homology detection, multiple sequence alignment strategies, postprocessing filtering procedures, and tree estimation methods. Specifically, three types of homologous loci (gene clusters) were used to develop our supermatrices, namely 1603 conserved

single-copy orthologs (CO), 1643 all single-copy orthologs (AO), and 4341 paralogy-parsed orthologs (PO) with  $\geq 42$  (~50%) species present (for more details, see Materials and Methods section). To date, our data represent the most comprehensive resource available for Odonata in terms of gene sampling. Each gene cluster was aligned, trimmed, and concatenated resulting in five main supermatrices, CO (DNA/AA), AO (AA), and PO (DNA/AA), which included 2,167,861 DNA (682,327 amino acid [AA] sites), 882,417 AA sites, 6,202,646 DNA (1,605,370 AA) sites, respectively. Thus, the largest alignment that we used to infer the odonate phylogeny consists of 4341 loci concatenated into a supermatrix with >6 million nucleotide sites. All supermatrices are summarized in Supplementary Table S2 available on Dryad; the inferred odonate relationships are shown in Supplementary Figure S1a available on Dryad whereas topologies of all inferred phylogenies are plotted in Supplementary Figure S1b available on Dryad and topologies of 1603 CO gene trees are shown in Supplementary Figure S1c available on Dryad. Additionally, we performed nodal dating of the inferred phylogeny using 20 fossil calibration points (Supplementary Table S3 available on Dryad).

The inferred ML phylogenetic tree of Odonata using DNA supermatrix of 1603 BUSCO loci (Fig. 1) was used as a primary phylogenetic hypothesis throughout this study as it agrees with the majority of relationships inferred by other methods (Supplementary Fig. S1a,b available on Dryad). Divergence of Zygoptera and Epiprocta (Anisozygoptera+Anisoptera) from the Most Recent Common Ancestor (MRCA) was estimated to have occurred in the Middle Triassic ~226 Ma (95% Credible Interval [CI]: 221.8–231.1 Ma, Fig. 1), which is in line with recent estimates (Thomas et al. 2013; Misof et al. 2014). Comprehensive phylogenetic coestimation of subordinal relationships within Odonata showed that the suborders were well supported (Supplementary Fig. S1a available on Dryad), as they were consistently recovered as monophyletic clades in all analyses. In several previous studies, paraphyletic relationships of Zygoptera had been proposed based on wing vein characters derived from fossil odonatoids and extant Odonata (Trueman 1996), analysis of 12S (Saux et al. 2003), analysis of 18S, 28S, Histone 3 (H3), and morphological data (Ogden and Whiting 2003) and analysis of 16S and 28S data (Hasegawa and Kasuya 2006). In most of these studies, Lestidae was inferred to be sister to Anisoptera. Functional morphology comparisons of flight systems, secondary male genitalia, and ovipositors also supported a nonmonophyletic Zygoptera with uncertain phylogenetic placement of multiple groups (Pfau 1991). Nevertheless, the relationships inferred from these previous data sets seem to be highly unlikely due to apparent morphological differentiation (e.g., eye spacing, body robustness, wing shape) between the suborders and support for monophyletic Anisoptera and Zygoptera from more recent morphological (Busse et al. 2015), molecular

(Carle et al. 2008; Thomas et al. 2013; Kim et al. 2014; Suvorov et al. 2017), and combined studies using both data types (Bybee et al. 2008). Our analyses recover Zygoptera as monophyletic consistently (Supplementary Fig. S1a available on Dryad).

Divergence time estimates suggest a TMRCA of Anisoptera and Anisozygoptera (we occasionally refer these two suborders as “Epiprocta”) in the Late Triassic (~204 Ma; 95% CI 201.7–207.8 Ma; Fig. 1). Epiprocta as well as Anisoptera were consistent with more recent studies and recovered as monophyletic with very high support. We also note here that our divergence time estimates of Anisoptera tend to be younger than those found by (Letsch et al. 2016). The fossil-calibration approach based on penalized likelihood that was used by (Letsch et al. 2016) has been shown to overestimate true nodal age (Britton et al. 2007) preventing direct comparison between our dates derived from the Bayesian framework MCMCTree and those estimated by (Letsch et al., 2016). Additionally, our divergence time estimate for Epiprocta is older than inferred by (Misof et al., 2014), which can be explained by the differences in calibration schemes. Specifically, for the Epiprocta crown node, we specified *Liassophlebia* sp. fossil using an informative skewed normal distribution prior (see Supplementary Table S3 available on Dryad).

The phylogenetic position of Gomphidae and Petaluridae, both with respect to each other and the remaining anisopteran families, has long been difficult to resolve. Several phylogenetic hypotheses have been proposed in the literature based on molecular and morphological data regarding the placement of Gomphidae as sister to the remaining Anisoptera (Blanke et al. 2013) or to Libelluloidea (Misof et al. 2001). Petaluridae has exhibited stochastic relationships with different members of Anisoptera, including sister to Gomphidae (Misof et al. 2001), sister to Libelluloidea (Carle et al. 2008), sister to Chlorogomphidae+Cordulegasteridae (Bybee et al. 2008), and sister to all other Anisoptera (Trueman 1996; Rehn 2003). The most recent analyses of the major anisopteran lineages using several molecular markers (Carle et al. 2015) suggest Gomphidae and Petaluridae as a monophyletic group, but without strong support. Here, the majority of our supermatrix analyses (Supplementary Fig. S1a available on Dryad) strongly support a sister relationship between the two families, and in our phylogeny (Fig. 1) they split from the MRCA ~161 Ma (95% CI: 156.6–165.5 Ma) in the Middle Jurassic (Fig. 1). We further investigated the species tree topologies that were estimated by the coalescent-based tree summary method, ASTRAL. We found that almost all these species trees reject such a relationship with high confidence (Supplementary Fig. S1a available on Dryad). In the presence of ILS, concatenation methods can be statistically inconsistent (Roch and Steel 2014) leading to an erroneous species tree topology with unreasonably high support (Kubatko and Degnan 2007). This inconsistency in the recovery

of a sister group relationship between Gomphidae and Petaluridae can be explained by elevated levels of ILS between the families and/or possible introgression events (Maddison 1997).

New zygopteran lineages originated in the Early Jurassic ~189 Ma (95% CI: 182.5–197.7 Ma) with the early split of Lestoidea and the remaining Zygoptera (Fig. 1). A subsequent occurrence of two large zygopteran groups, Calopterygoidea and Coenagrionoidea, was estimated within the Cretaceous (~67 Ma; 95% CI: 61.5–71.6 Ma and 115.8 Ma; 95% CI: 112.7–121.2 Ma for Calopterygoidea and Coenagrionoidea, respectively) and culminated with the rapid radiation of the majority of extant lineages in the Paleogene in the interval between ~23 and ~66 Ma. Our calibrated divergences generally agree with estimates in (Thomas et al. 2013). However, any further comparisons are precluded by the lack of comprehensive divergence time estimation for Odonata in the literature. The backbone of the crown group Calopterygoidea that branched off from Coenagrionoidea ~129 Ma (95% CI: 121.9–134.8 Ma) in the Early Cretaceous was well supported as monophyletic in most of our inferred phylogenies (Fig. 1 and Supplementary Fig. S1a available on Dryad). Previous analyses struggled to provide convincing support for the monophyly of the superfamily (Bybee et al. 2008; Carle et al. 2008; Dijkstra, Kalkman et al. 2014), whereas only 11 out of 48 phylogenetic reconstructions rejected Calopterygoidea (Supplementary Fig. S1a available on Dryad).

We used QS (Pease et al. 2018) to provide additional information about nodal support and investigate biological explanations for alternative evolutionary histories that received some support. We found that for most odonate key radiations, the majority of quartets (i.e. Frequency >0.5) support the proposed phylogenetic hypothesis with QC scores >0 (Supplementary Fig. S2 available on Dryad) across all estimated putative species trees (Supplementary Fig. S1b available on Dryad). The few exceptions consist of the Gomphidae+Petaluridae split and the A+B split, where we have Frequency <0.5 and QC <0, which suggests that alternative relationships are possible. QD, inspired by  $f$  and  $D$  statistics for introgression, provides an indicator of how much the proportions of discordant quartets are skewed (i.e. whether one of the two discordant relationships is more common than the other), suggestive of introgression and/or substitution rate heterogeneity (Pease et al. 2018). Interestingly, we identified skewness (i.e. QD <0.5) for almost every major radiation (Supplementary Fig. S2 available on Dryad), which suggests that alternative relationships can be a result of additional underlying processes (e.g. introgression) rather than ILS alone (Pease et al. 2018); however, this score may not be highly informative if the majority of quartets agree with the focal topology (i.e., Frequency >0.5 and QC >0). For both the Gomphidae+Petaluridae and the A+B splits, we have Frequency >0.5, QC <0, and QD <0.5, implying that alternative phylogenetic relationships are plausibly not only due to ILS but also possible ancestral introgression.



### Major Trends in Evolutionary History of Odonata

Investigation of diversification rates in Odonata highlighted two major trends correlated with two mass extinction events in the Permian-Triassic (P-Tr) ~251 Ma and Cretaceous-Paleogene (K-Pg) ~66 Ma. First, it appears that P-Tr mass extinction event might have reduced the extent of biodiversity that had been present in Odonata as reflected in the fossil record (Rohde and Muller 2005) for that period (see the temporal distribution of fossil samples in Fig. 1) as was also the case for multiple insect lineages (Labandeira and Sepkoski 1993). According to the fossil record, at least two major odonatoid lineages went extinct (Protodonata and Protanisoptera; Grimaldi and Engel 2005) and likely many genera from other lineages as well (e.g., Kargalotypidae from Triadophlebimorpha; Nel et al. 2001). The establishment of major odonate lineages was observed during the Cretaceous starting ~135 Ma (Fig. 1, red line). This coincided with the radiation of angiosperm plants that, in turn, triggered the formation of herbivorous insect lineages (Misof et al. 2014). Odonates are exclusively carnivorous insects, and their diversification was likely driven by the aforementioned sequence of events. Interestingly, molecular adaptations in the odonate visual systems are coupled with their diversification during the Cretaceous as well (Suvorov et al. 2017).

### Overview of Introgression Hypotheses Tested

The scope of introgression within Odonata remains largely unknown, where previous studies looked for its patterns only within certain species relying on inference from a limited number of genetic loci. Thus, we searched for signatures of introgression using genome-scale data sets between lineages at several different taxonomic levels: between different suborders, between superfamilies, and within superfamilies. We used six different methods to test for introgression within Odonata, as exemplified for the Anisozygoptera suborder in Figure 2. Specifically, we searched for signatures of ancestral inter-superfamilial introgression within the Zygoptera and Anisoptera suborders. Also, we tested the hypothesis of inter-subordinal gene flow between Anisozygoptera and Zygoptera. Finally, we tested introgression within superfamilies of Zygoptera and Anisoptera that included several species (Lestoidea, Calopterygoidea, Coenagrionoidea, Aeshnoidea (Aeshnidae), Aeshnoidea (Gomphidae+Petaluridae), Cordulegastroidea, and Libelluloidea; Fig. 1). The introgression results for the entire Odonata order either comprise of all tests performed within the entire phylogeny (HyDe/ $D$ ) or of a union of tests performed within Anisoptera, Zygoptera, and between Anisozygoptera-Zygoptera ( $D_{FOIL}$ , QuiBL, and  $\chi^2$  count test/BLI).

### Site Pattern-Based Methods Strongly Suggest Multiple Instances of Introgression within Odonata

Initially, we tested the above hypotheses of introgression in quartet topologies (Supplementary Fig. S3 available on Dryad) within Odonata using two site pattern-based methods: the ABBA-BABA test (Patterson et al. 2012) and HyDe (Meng and Kubatko 2009). The ABBA-BABA test and HyDe rely on computation of  $D$  and  $\gamma$  statistics, respectively, where their significant deviation from 0 may indicate the presence of introgression between the tested pair of taxa. Additionally, estimated  $\gamma$  and  $(1-\gamma)$  of HyDe's hybrid speciation model (Meng and Kubatko 2009) corresponds to the parental fractions in a putatively hybrid genome. Note that HyDe's hybrid speciation model is appropriate for detecting introgression with sufficient statistical power and can produce reasonable estimates of  $\gamma$  (Blischak et al. 2018; Kong and Kubatko 2021). The analysis of the ABBA-BABA test results revealed possible gene flow events throughout the entire evolutionary history of Odonata (Supplementary Table S5, Fig. S4a and Results available on Dryad). We also highlight the positive relationship between the values of  $D$  and  $\gamma$  statistics (Spearman's rank correlation test,  $\rho = 0.308$ ,  $P = 0$ ), demonstrating their broad concordance in identifying signatures of introgression (Supplementary Fig. S4b available on Dryad).

There are a variety of other test statistics that have been developed to detect introgression (e.g., Green et al. 2010; Durand et al. 2011; Martin et al. 2015; Kubatko and Chifman 2019). Because, like  $D$  and  $\gamma$ , many of these statistics are computed from different invariants, we attempted to visualize the relationships between all 15 site patterns computed by HyDe using  $t$ -distributed stochastic neighbor embedding (tSNE; van der Maaten and Hinton 2008) for dimensionality reduction, along with the corresponding values of  $D$  and  $\gamma$  (Supplementary Fig. S4c,d available on Dryad, respectively). We found that the clustering of quartets with significant introgression according to a two-dimensional representation of their site patterns may suggest the presence of additional site pattern signatures of introgression (Supplementary Fig. S4c,d available on Dryad). These results suggest that powerful dimensionality reduction techniques could serve as a useful tool for the exploration and visualization of complex signatures of introgression simultaneously estimated from a large set of site patterns.

In order to assess the extent of preservation of ancestrally introgressed genetic material within contemporary taxa, we compared inferred average values of significant  $\gamma$  statistic from Odonata with the averages derived from different intra- and inter-superfamilial taxonomic levels (Fig. 3a). We found significantly higher values of  $\gamma$  for several intra- and inter-superfamilial comparisons including those that involve Anisozygoptera (Wilcoxon rank-sum test [WRST], all  $P < 0.05$ , Fig. 3a, Supplementary Table S5 and Results available on Dryad). Additionally,

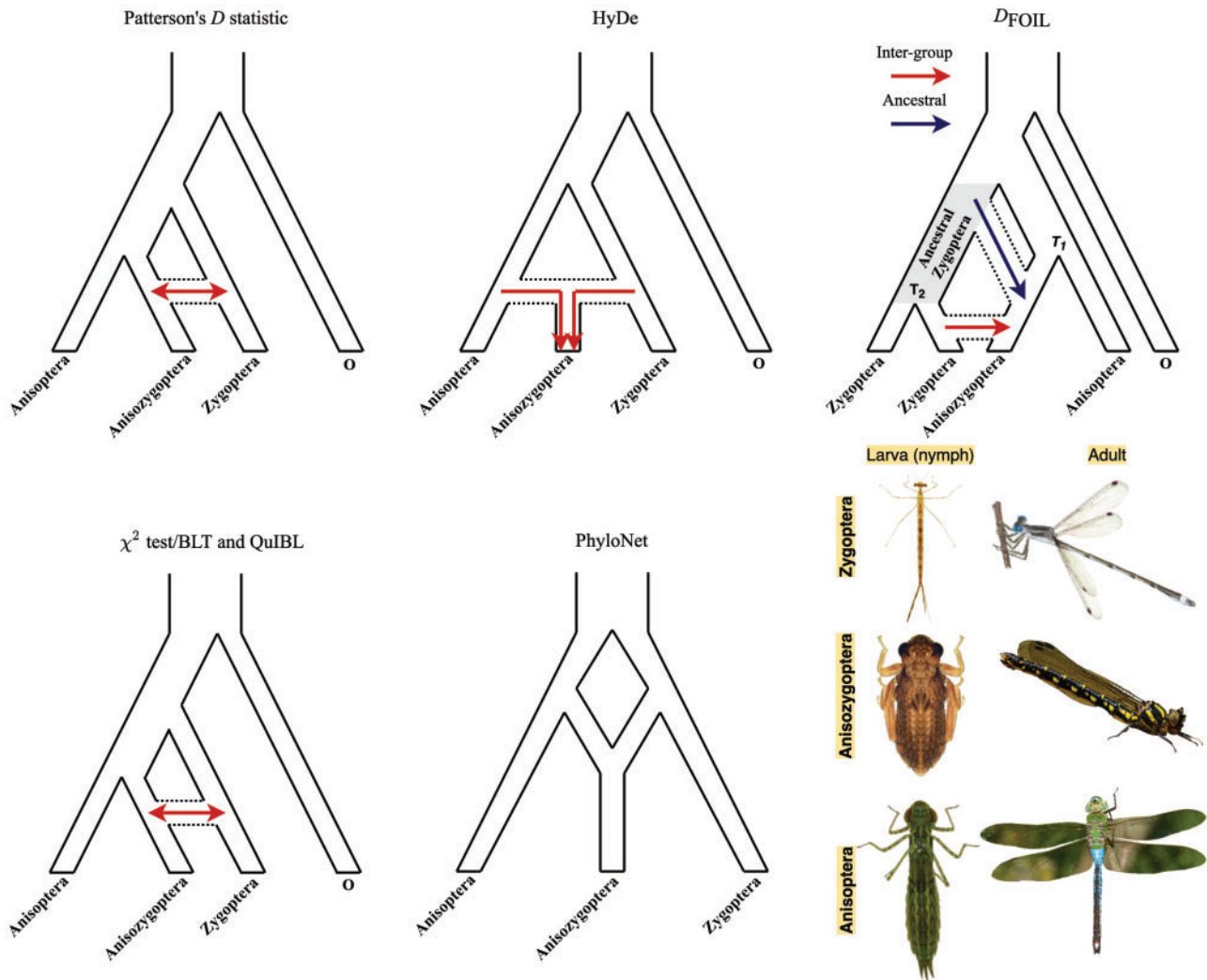


FIGURE 2. Detection of introgression/hybridization trajectories by different methods in Anisozygoptera. Three site pattern-based ( $D$  statistic, HyDe, and  $D_{FOIL}$ ), gene tree count/branch length-based ( $\chi^2$  test/BLT and QuIBL), and network ML inference (PhyloNet) methods were used to test for introgression/hybridization. Arrows denote introgression. The figure panel represents larval and adult stages for three Odonata suborders. Species from top to bottom: *Lestes australis*, *Epiophlebia superstes*, and *Anax junius*. Image credit: *Epiophlebia superstes* adult by Christian Dutto Engelmann; *L. australis*, and *A. junius* adults by John Abbott.

Anisozygoptera exhibits the largest average  $\gamma$  (0.27) across all the inter-superfamilial comparisons (Fig. 3a, Supplementary Table S5 available on Dryad). We also found an excess (Fisher exact test [FET], all  $P < 0.05$ , Supplementary Table S5 available on Dryad) of significant triplets that support introgression (Fig. 3b) based on both the ABBA-BABA and HyDe hybrid speciation model (Supplementary Fig. S3 available on Dryad) tests for Anisozygoptera, Aeshnoidea (Aeshnidae), Lestoidea, and Calopterygoidea (between and within). We note that the accuracy of introgression detection for site pattern-based methods may be impaired by saturation, which will be exacerbated on larger timescales. Thus, we additionally performed HyDe analysis using only the 1st and 2nd codon positions and obtained highly similar results for  $D$  and  $\gamma$  (Supplementary Fig. S5 available on Dryad) suggesting

that the potential saturation effect in 3rd codon position did not severely impact our inferences. Despite these results, the  $D$  statistic distributions, if considered individually, should be interpreted with caution: the ABBA-BABA test can produce false positives within genomic regions of reduced interspecific divergence, and can also be significantly affected by demographic parameters, genetic drift, and variation in recombination rates (Martin et al. 2015).

Furthermore, we tested introgression within Odonata using an alternative site pattern-based method,  $D_{FOIL}$  (Supplementary Fig. S6a and Results available on Dryad), which is capable of detecting ancestral as well as intergroup introgression and inferring its polarization (see Materials and Methods section). Specifically, we observed a highly skewed distribution of  $D_{FOIL}$  statistics for Anisozygoptera (Supplementary

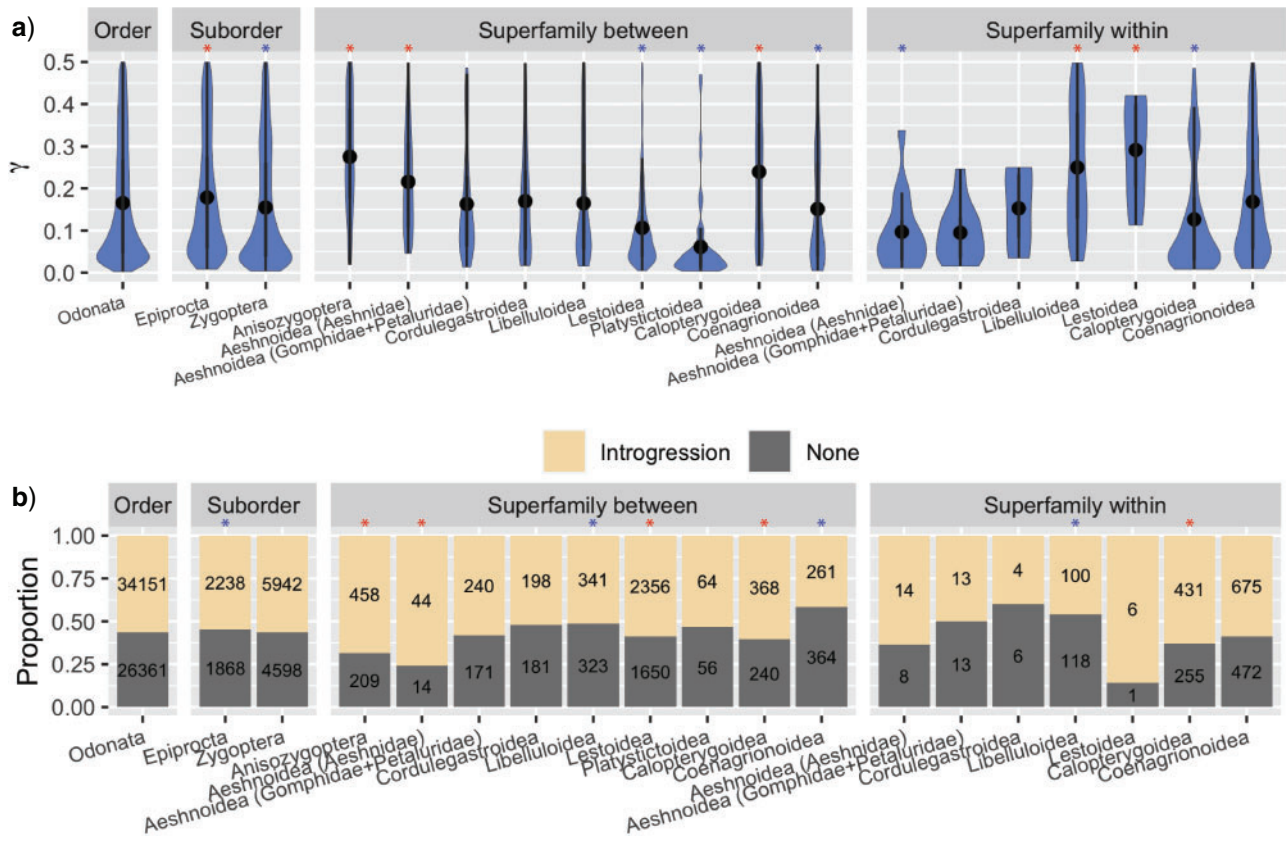


FIGURE 3. Distributions of HyDe and quartets fractions supporting introgression across odonate taxonomic levels. a) Distribution of significant (Bonferroni corrected  $P < 10^{-6}$  values for each quartet estimated by HyDe. In general,  $\gamma$  values that are not significantly different from 0 denote no relation of a putative hybrid species to either of the parental species P1 ( $1-\gamma$ ) or P2 ( $\gamma$ ) in a quartet. Asterisks indicate significantly greater (red) or lower (blue) averages of various tested cases compared to average of the entire order. b) Proportions of quartets that support introgression based on simultaneous significance of D statistics and  $\gamma$ . Asterisks indicate significantly greater (red) and smaller (blue) fraction of quartets that support introgression compared to the entire order.

Fig. S6b and Results available on Dryad) that may suggest specific directionality of introgression: all 61 (1157 out of 1158 without FDR correction) quintets with positive evidence for ancestral introgression suggest that Anisozygoptera is the recipient lineage whereas Zygoptera is the donor (Fig. 2, red and blue arrows). Additionally, 1030 out of 1091 (4473 out of 4738 without FDR correction) evaluated quintets with significant intergroup introgression are indicative of one-way introgression from Zygoptera lineages to Anisozygoptera as well, whereas the directionality of remaining 59 (254 without FDR correction) quintets support Anisozygoptera as a donor and Zygoptera as a recipient and only two (11 without FDR correction) show introgression between Zygoptera and Anisoptera.

#### Signatures of Introgression Revealed by Phylogenetic Gene Tree-Based Discordance Methods

Besides specific site patterns, introgression will also generate certain patterns of gene tree-species tree discordance and reduce the genetic divergence between introgressing taxa, which is reflected in gene tree branch lengths. Thus, the footprints of introgression can be

detected using phylogenetic discordance methods. First, for a triplet of species, under ILS alone one would expect equal proportions of gene tree topologies supporting the two topologies disagreeing with the species tree, and any imbalance may suggest introgression (Supplementary Fig. S7 available on Dryad). Thus, deviation from equal frequencies of gene tree counts among discordant gene trees can be assessed using a  $\chi^2$  test, similar to previously proposed methods leveraging discordant gene tree counts (Huson et al. 2005; Degnan and Rosenberg 2009). One would expect the average distance between putatively introgressing taxa in discordant trees to be significantly smaller than the distances derived from the concordant as well as alternative discordant triplets (see Materials and Methods section and Supplementary Fig. S7 available on Dryad). We used both the  $\chi^2$  test of discordant gene tree counts and a test based on the distribution of branch lengths for concordant and discordant gene tree triplets (BLT) to identify introgression within Odonata testing different scenarios (Fig. 4a). With this combination of methods, we identified a significant fraction of triplets that support ancestral introgression for scenario 1 that involves

inter-subordinal gene flow between Anisozygoptera and Zygoptera as well as scenarios 2 through 4, which correspond to inter-superfamilial instances of introgression within Epiprocta (Fig. 4b). Within superfamilies, we found signatures of introgression for Calopterygoidea and Libelluloidea (Fig. 4b). For scenario 1 (introgression between Zygoptera and Anisozygoptera), examination of the genetic divergence distributions (Fig. 4c) for concordant and discordant triplets showed that discordant triplets that may have resulted from gene flow between Anisozygoptera and Zygoptera (the topology labeled “discord2”), have markedly smaller average divergence between these two taxa, as expected in the presence of introgression. Similarly, based on the distribution of mean divergence between putatively introgressing taxa (Supplementary Fig. S8 available on Dryad) as well as fraction of significant triplets (Fig. 4b) gene flow is supported for scenarios 2, 3, and 4.

Additionally, we used a gene tree branch length-based approach, QuIBL (Edelman et al. 2019), which also detected multiple instances of introgression within the entire order (Supplementary Fig. S9 available on Dryad). We note that particularly for introgression involving Anisozygoptera we observed a larger fraction of triplets suggestive of introgression than for any other scenario tested.

#### *Phylogenetic Network Analyses Support Anisozygoptera-Zygoptera Introgression*

As an alternative approach to identify the lineage experiencing gene flow with Anisozygoptera, we performed phylogenetic network inference in PhyloNet (Than et al. 2008; Wen et al. 2018). For this analysis, we specified that Anisozygoptera was involved in a reticulation event—the only such event occurring on the tree—and inferred for the other two nodes that were most likely to be involved in the reticulation as well as the value of  $\gamma$ , the fraction of Anisozygoptera’s genetic material derived from this reticulation. The full maximum likelihood (Fig. 4d) and maximum pseudolikelihood (Supplementary Fig. S10 available on Dryad) approaches recovered topologically similar networks with comparable values of  $\gamma$ . Pseudolikelihood analysis suggests a reticulation event between Aeshnidae (a family within Anisoptera) and Zygoptera with 38% of genetic material coming from Zygoptera (Supplementary Fig. S10 available on Dryad), whereas full likelihood infers reticulation between Anisoptera and Zygoptera suborders 33% (Fig. 4d) of genetic material from Zygoptera. Overall, we note that the full likelihood approach returned networks with higher log-likelihood scores. This observation is most likely due to the fact that we performed full likelihood analysis in an exhaustive manner (Supplementary Table S4 available on Dryad) testing every possible reticulation event within a focal clade topology congruent with the species tree (Fig. 1), whereas pseudolikelihood analysis used

the hill-climbing algorithm to search the full network space but is not guaranteed to retrieve the most optimal solution. Moreover, differences in objective function within likelihood and pseudolikelihood frameworks could also lead to distinct network topologies and  $\gamma$  estimates.

#### DISCUSSION

Using a comprehensive multi-locus transcriptomic data set, we reconstructed a fossil-calibrated deep evolutionary history of dragonflies and damselflies (Odonata; Fig. 1). Although our phylogenetic analyses resolve many major radiations within the order with high confidence, we note that a strictly bifurcating phylogeny could be positively misleading (i.e. asserting erroneous relationships with high support) or provide a poor fit for genomic data undergoing biological processes such as ILS and introgression, respectively. Thus, the phylogenies presented in this paper should be interpreted with a degree of caution. Untangling patterns of phylogenetic discordance within our data set revealed multiple gene flow events that have been impacted the course of Odonata evolution for the past 200 myr. We examined the agreement across site- and gene tree-based methods for detecting introgression (i.e., HyDe/*D*, and *D*<sub>FOIL</sub> and the  $\chi^2$  test/BLT; Fig. 5 and Supplementary Fig. S11 available on Dryad). Overall, all methods individually were able to identify abundant introgression within the entire Odonata order with strong agreement. We found considerable overlap across methods in their support of introgression within Epiprocta (scenarios 2 and 3), gene flow involving Anisozygoptera (scenario 1), and intra-superfamilial introgression within Libelluloidea. Within Zygoptera, our methods showed strong overlap in identifying signatures of introgression for Calopterygoidea only. Notably, our  $\chi^2$  test/BLT produced very few predictions that were not in agreement with HyDe, *D*, and/or *D*<sub>FOIL</sub> across different comparisons. Our deep-time introgression analyses suggest that ancestral introgression events may leave genetic footprints that are preserved in the genomes and observed in the phenotypes of contemporary species. Below, we discuss the implications of our phylogenetic results in the context of previous studies in Odonata, before turning to the importance and challenges associated with the detection and interpretation of signatures of introgression within phylogenomic studies in light of our findings.

#### *Major Radiations on Odonata Phylogeny*

Several competing hypotheses of evolutionary relationships within Odonata have been proposed by multiple authors regarding various taxonomic levels (Supplementary Fig. S12a available on Dryad; Trueman 1996; Misof et al. 2001; Saux et al. 2003;

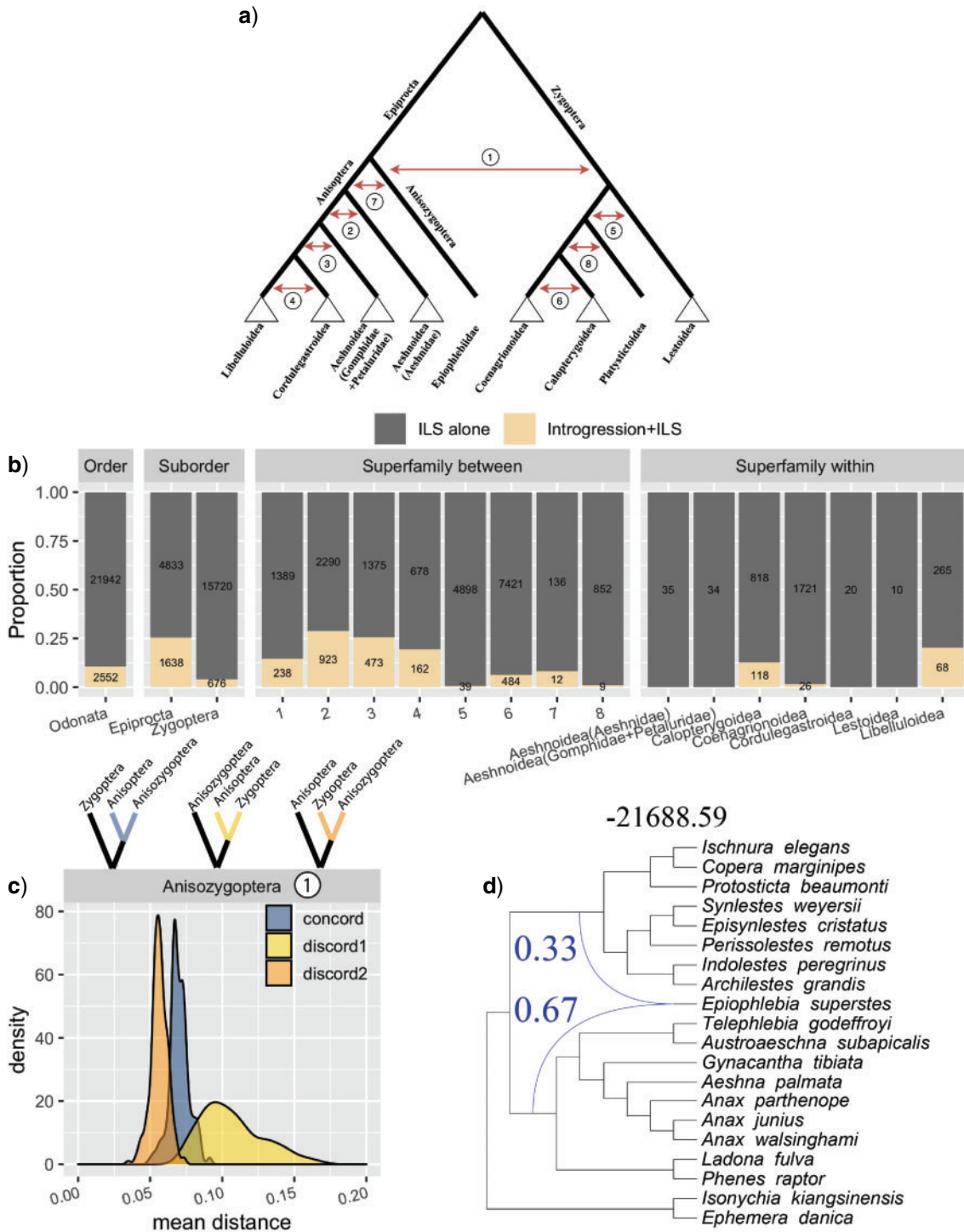


FIGURE 4. Results of the  $\chi^2$  Count-BLT for Odonate Taxonomic Levels and PhyloNet result for Anisozygoptera. a) Scenarios of deep (numbered red arrows) and intra-superfamilial (white triangles) introgression in Odonata tested using  $\chi^2$  test and BLT. Red arrows mark the location of ancestral introgression events that were tested between lineages (e.g. for scenario 8, we tested whether contemporary species of Platystictoidea shared introgressed genetic material with either Coenagrionoidea or Calopterygoidea). b) Classification of triplets based on the  $\chi^2$  test and BLT results. Introgression+ILS cases are those significant according to both the  $\chi^2$  test and BLT (FDR corrected  $P < 0.05$ ); all the remaining cases were those where any discordance was inferred to be due to ILS alone. c) Normalized genetic divergence between sister taxa (shown in triplets above the panel) averaged across all BUSCO gene trees supporting each topology involving three lineages representing Anisoptera, Anisozygoptera, and Zygoptera. d) Phylogenetic network estimated from a set of ML gene trees using maximum likelihood. *Epiophlebia superstes*, the sole representative of Anisozygoptera in our study, was specified to be involved in a reticulation with two other (unspecified) lineages. Blue lines indicate the reticulation event and are labeled with PhyloNet's estimate of  $Y$ . The number above the network indicates the log-likelihood score.

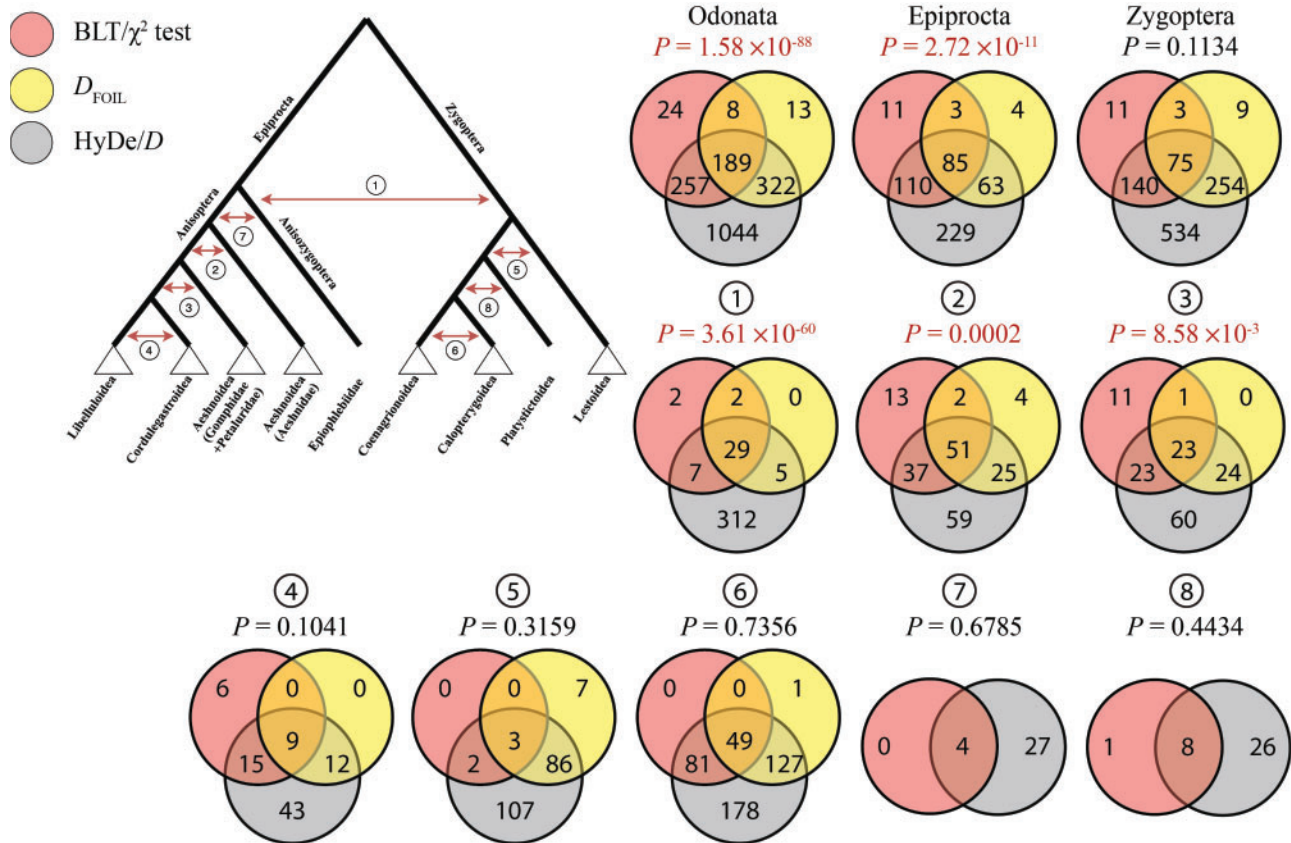


FIGURE 5. Overlap between putatively introgressed species pairs inferred by HyDe/D,  $D_{FOIL}$ , and BLT/ $\chi^2$  test. The tree shows tested scenarios of deep (numbered red arrows) introgression for Anisoptera, Anisozygoptera, and Zygoptera. The numbers within sets represent the number of unique introgressing species pairs identified by a corresponding method. Significance of an overlap between all methods (intersection of all sets) for each scenario was determined by the exact multiset interactions test. Significant  $P$ -values are indicated in red. Note that due to the limitations of  $D_{FOIL}$ , introgression could not be tested for scenarios 7 and 8 using this method.

Hasegawa and Kasuya 2006; Ware et al. 2007; Bybee et al. 2008; Carle et al. 2008, 2015; Dumont et al. 2010; Blanke Greve et al. 2013; Dijkstra, Kalkman et al. 2014; Suvorov et al. 2017). Our phylogenetic analyses recovered Epiprocta (Anisoptera+Anisozygoptera) and Zygoptera as monophyletic with high support (Supplementary Fig. S1a available on Dryad) agreeing with other recent studies (Bybee et al. 2008; Carle et al. 2008; Dumont et al. 2010; Suvorov et al. 2017). Our estimated superfamilial relationships within Zygoptera support hypothesis of Dijkstra, Kalkman et al. (2014) recovering monophyly of Lestoidea, Platystictioidea, Coenagrionoidea, and Calopterygoidea (Supplementary Fig. S12b available on Dryad) with high support (Supplementary Fig. S1a available on Dryad). Inferred higher-level phylogenetic classification of anisopteran families was highly congruent with (Carle et al. 2015) and well-supported (Supplementary Fig. S1a available on Dryad) with the exception of Gomphidae and Petaluridae radiations. The phylogenetic position of Gomphidae and Petaluridae, both with respect to each other and the remaining anisopteran families, has long been difficult to resolve (Supplementary Fig. S12c available on Dryad). The most recent analyses of major anisopteran lineages, using

several molecular markers (Carle et al. 2015), suggest Gomphidae and Petaluridae as a monophyletic group, but without strong branch support.

The multispecies coalescent model (MSC) provides a probabilistic framework for estimation of species trees that accounts for genealogical discord occurring as a result of ILS. Close scrutinization of Gomphidae and Petaluridae relationships inferred under concatenation and ASTRAL (a supertree method that is statistically consistent under MSC) showed that the majority of the supermatrix analyses strongly support a sister relationship between the two families (Supplementary Fig. S1a available on Dryad); however, almost all the ASTRAL species tree analyses reject such a relationship with high confidence (Supplementary Fig. S1a available on Dryad). In the presence of ILS concatenation methods can be statistically inconsistent (Roch and Steel 2014) leading to an erroneous species tree topology with unreasonably high support (Kubatko and Degnan 2007). Thus, inconsistency in the recovery of a sister group relationship between Gomphidae and Petaluridae between concatenation and ASTRAL could be a result of elevated levels of ILS between the families. Furthermore, gene tree-species tree conflict

can occur in the presence of nonsister species gene flow (Leaché et al. 2014), which violates assumptions of the MSC by skewing frequency distributions of incongruent gene tree topologies thereby making the MSC framework inconsistent for species tree estimation (Eckert and Carstens 2008; Solís-Lemus et al. 2016), although we note that studies of this phenomenon have examined gene flow at shallower phylogenetic timescales than those investigated here. We found that the Gomphidae and Petaluridae lineages exhibited inter-superfamilial introgression events (scenario 3, Fig. 5) involving the Cordulegastroidea + Libelluloidea clade. Additionally, the familial relationships within Calopterygoidea significantly varied between estimated phylogenies using either ASTRAL or concatenation methods (Supplementary Fig. S1a available on Dryad). For example, within clade C, monophyly of the Calopterygoidea and Chlorocyphidae families was suggested by ASTRAL trees but rejected by the majority of ML phylogenies estimated from the supermatrices (Fig. 1 and Supplementary Fig. S1a available on Dryad). Interestingly, for this superfamily further analyses similarly yielded abundant instances of interfamilial introgression (Fig. 5). Together, these results may support the proposition that purely bifurcating species topologies inferred under concatenation/MS methods in the presence of postspeciation introgression on recent as well as deep temporal scales may inadequately model taxonomic relationships (Fontaine et al. 2015; McVay et al. 2017; Zhang et al. 2021). To alleviate this problem, a unifying multispecies coalescent network model, implemented in the program PhyloNet (Yu et al. 2011), has been developed to describe evolutionary history via species networks where reticulation nodes correspond to instances of introgression. Unfortunately, we were not able to infer a full species network topology using PhyloNet because the taxon and gene sampling presented in our study would render this analysis unfeasible even when using the more tractable pseudolikelihood implementation (Yu and Nakhleh 2015). However, we were able to use PhyloNet to test patterns of reticulate evolution involving Anisozygoptera (see below).

We also note that discordance caused by ILS, if not accounted for, may lead to inaccurate inference of substitution rates (Mendes and Hahn 2016) and thus overestimation of divergence times using relaxed clock models (Ogilvie et al. 2016). Moreover, a failure to incorporate introgression effects into a probabilistic framework of a time calibration method will result in underestimated divergence times (Leaché et al. 2014). Several recent fully Bayesian approaches have been proposed to perform divergence time estimation using the MSC model alone (Heled and Drummond 2010; Ogilvie et al. 2017) or together with introgression (Jones 2019), however, they would not be scalable to our data set.

#### *Widespread Introgression within Odonata*

Introgression among Odonata has been previously thought to be uncommon (Tennesen 1982; Lowe et al. 2008) as a result of probable reproductive isolation mechanisms such as ethological barriers, phenotypic divergence (e.g., variable morphology of genitalia; Hosken and Stockley 2004; Barnard et al. 2017) and habitat and temporal isolation. Most of the introgression and hybridization research in Odonata has been done within the zygopteran Coenagrionidae family and especially between populations of genus *Ishmura* focusing on mechanisms of reproductive isolation (e.g. Sanchez-Guillen et al. 2011; Sanchez-Guillen et al. 2014). These studies established “hybridization thresholds” for these closely related species and showed positive correlation between isolation and genetic divergence. Furthermore, rapid karyotype evolution can also contribute to postmating isolation (Lai et al. 2005); however, recent cytogenetic studies across Odonata phylogeny indicate very stable chromosome number with most prevalent karyotype of  $2n = 25$  (Kuznetsova and Golub 2020). Additionally, in recent years, there has been a growing body of evidence for introgression throughout evolutionary histories of various groups. This includes more recent hybridization events observed in *Heliconius* butterflies (Edelman et al. 2019), cats (Li et al. 2016), cichlid fishes (Svardal et al. 2020) as well as deeper ancestral introgression in primates (Vanderpool et al. 2020), *Drosophila* (Suvorov et al. 2021), and vascular plants (Pease et al. 2018).

The extent of gene flow and maintenance of introgressed variation together determine the fraction of introgressed material, or  $\gamma$ , in a focal genome (Martin and Jiggins 2017). However, with increased divergence time the fixation or loss of the ancestrally introduced genetic material will primarily depend on the strength and direction of selection (Norris et al. 2015; Oziolor et al. 2019; Petr et al. 2019). Here, our taxon sampling allowed to test ultra-deep ancestral introgression scenarios where the MRCA of tested taxa can be traced as far back as to the Triassic period (~251 to ~201 Ma). We argue that for the cases where we infer that a large amount of introgressed genetic material was preserved (e.g. >25% in Anisozygoptera) the ancestral effective migration rates (Martin and Jiggins 2017) were high (similar conclusions can be made for Aeshnoidea (Aeshnidae), Calopterygoidea and within Libelluloidea and Lestoidea; Fig. 3a); whereas for the remaining taxa with lower or nonsignificant deviations of  $\gamma$  (Fig. 3a), the rates of introgression may have been substantially lower or its signatures were purged from the genome by selection.

We found compelling evidence for patterns of ancestral introgression (Fig. 5) among distantly related odonate taxa. Our conservative analysis of agreement between different introgression tests shows the presence of gene flow within the entire order (Fig. 5 and Supplementary Fig. S11 available on Dryad). This observation may be explained by reduced sexual

selection pressures in the early stages of odonate evolution that may have inhibited rapid genital divergence (Eberhard 2004), which is probably a primary source of reproductive isolation in Odonata (Cordero Rivera et al. 2004).

#### *Phenotypic Consequences of Deep Time Introgression*

Perhaps the most compelling evidence that we uncovered in this study was for deep ancestral introgression between the Zygoptera and Anisozygoptera suborders, which based on the fossil record most likely became genetically isolated after the Lower Jurassic (Carle 2012). Species of Anisozygoptera exhibit anatomical characteristics of both Anisoptera and Zygoptera suborders. Some general features of Anisozygoptera that relate them to Zygoptera include dorsal folding of wings during perching in adults, characteristic anatomy of proventriculus (a part of digestive system that is responsible for grinding of food particles), and absence of specific muscle groups in the larval rectal gills; whereas abdominal tergite shape, rear wing geometry and larval structures are similar to Anisoptera (Asahina et al. 1954). More recent studies also revealed that Anisozygoptera ovipositor morphology shares similarity with Zygoptera (Matushkina 2008); muscle composition of the head resemble characteristics of both Anisoptera and Zygoptera (Blanke et al. 2013); thoracic musculature of Anisozygoptera larva exhibit similarity between Anisoptera and Zygoptera (Busse et al. 2015). Thus, Anisozygoptera represent a morphological and behavioral “intermediate” (Liu et al. 2011), which is supported by our findings where we recovered strong evidence of introgression between Zygoptera and Anisozygoptera (Figs. 2–4). Moreover, according to the  $D_{FOIL}$  method the Anisozygoptera was inferred to be a recipient taxon from a zygopteran donor, though we cannot rule out a lesser degree of gene flow in the opposite direction as well. In fact, such a phenotypic “intermediate” can occur as a result of homoploid hybrid speciation (Elgvin et al. 2017), which generates recombinant (mosaic) genotypes from two parental genomes while preserving their ploidy. For example, empirical studies have suggested that sex chromosome mosaicism in hybrid tiger swallowtail butterflies was linked to phenotypic mosaicism (e.g. female dimorphism and duration of a life cycle; Kunte et al. 2011), and that hybrid speciation is the cause of an intermediate plumage phenotype in sparrows (Hermansen et al. 2011). A significant fraction of genetic material from both parental genomes is one of the main conditions required to establish hybrid speciation (Schumer et al. 2014). Strikingly, we found that the average HyDe probability parameter  $\gamma \sim 0.27$  (Fig. 3a) inferred from multiple quartets is very similar to PhyloNet’s inheritance probability  $\gamma \sim 0.33$ . This may suggest that a sizeable fraction of the Anisozygoptera genome descends from zygopteran lineages. However, we note that genetic mosaicism and intermediate traits

can be also acquired via postspeciation gene flow (vonHoldt et al. 2011; Bonfante et al. 2021). Thus, to fully test the Anisozygoptera hybrid speciation hypothesis the other two conditions need to be examined: 1) the presence of reproductive barriers between hybrid and parental lineages and 2) the establishment of reproductive isolation was caused by hybridization events (Schumer et al. 2014). It is impossible to empirically test these conditions for gene flow events as ancient as the one we identified for Anisozygoptera.

Taken together, our observations strongly suggest a xenoplasious origin (Wang Y. et al. 2020) of Anisozygopteran traits (i.e. traits introduced to a recipient taxon via introgression) that are shared with Zygoptera. However, we do not reject the possibility that some trait hemiplasy may have resulted from ILS (Guerrero and Hahn 2018). Based on the gathered evidence for introgression, we suggest that ancestral lineages that gave rise to modern-day Anisozygoptera and Zygoptera experienced introgression in their past evolutionary history.

According to the hybrid swarm hypothesis (Seehausen 2004), introgression can trigger a rapid cladogenesis resulting in the establishment of ecologically different species with niche-specific adaptive phenotypes. Some of the notable examples can include adaptive radiations caused by ancestral introgression in cichlid fishes (Meier et al. 2017), and intricate interspecific introgression patterns in big cats that could be linked to rapid diversification of modern-day species in that lineage (Figueiro et al. 2017). Interestingly, the large fraction of introgressed material estimated within the Anisozygopteran lineage does not appear to have facilitated any adaptive radiation. This proposition is supported by an extremely low species diversification within the suborder (just three extant species) and also by the lack of fossil record for Anisozygoptera.

#### CONCLUSIONS

A rapidly growing body of empirical evidence strongly indicates that introgression is a widespread phenomenon observed not only in plants but also in the animal kingdom. Over the past decade, this biological process has received tremendous attention from the phylogenetics community, as it fundamentally changes how we view and reconstruct evolutionary histories of different organisms and may even redefine our understanding of species concepts (Wang X. et al. 2020). Introgression is an important source of novel variation that can lead to speciation, trigger rapid species diversifications, facilitate adaptation to novel environments (Nolte and Tautz 2010) as well as affect the course of species boundary establishment (Harrison and Larson 2014). From a practical perspective, introgression is one of the key factors that need to be considered during the development of biodiversity protection and conservation programs (Quilodr an et al. 2020). Furthermore, a failure to accurately detect introgression



scenarios may also lead to ineffective domestication and breeding programs (Dempewolf et al. 2017; Glémin et al. 2019; Janzen et al. 2019).

Here, we investigated a unique and ancient insect lineage, Odonata, and provided the first insight into global patterns of introgression that were pervasive throughout their evolutionary history. Moreover, we note that signatures of introgression were most likely underestimated as majority of phylogenomic methods (including those used in the current study) are unable to detect gene flow between sister lineages (Hibbins and Hahn 2021). Our findings further exemplify the evidence that postspeciation gene flow can be a fairly common process occurring in various taxa, including the most diverse group of animals, that is insects. The abundance of this biological phenomenon across the Tree of Life creates patterns of reticulate evolution which make the tree model itself ill-suited for explaining historic relationships between species (Doolittle and Bapteste 2007). It is possible that ancestral sequence reconstruction methods may also be affected by introgression as they typically assume character evolution along a single species tree (Mendes and Hahn 2016). Additionally, introgression poses new challenges for phylogenetic time calibration by biasing age estimates (Leaché et al. 2014). The fraction of the introgressed variation from a donor to a recipient taxon can vary significantly (Runemark et al. 2019), including cases where the most of the ancestry originates from donor genomes (Fontaine et al. 2015). In our case, we show that in Odonata introgressed genetic material can account for a large fraction of the genome (around ~30% in Anisozygoptera) and persist for millions of years following the gene flow event(s). This pattern is indicative of a high rate of gene flow and potentially of positive selection in favor of some hybrid genotypes.

We provide a roadmap of analyses to help identify introgression at both shallow and deep phylogenetic scales that is practical, timely, and much needed. Our research highlights the importance of development of tractable models and methods that scale to modern phylogenomic data sets derived from high-throughput molecular data. Moreover, we argue there is an urgent need to develop a theoretical framework that unifies various sources of phylogenetic discordance for more accurate and comprehensive inferences in phylogenetics (Charles-Elie et al. 2020).

#### DATA AVAILABILITY

All raw RNA-seq read libraries generated for this study have been uploaded to the Short Read Archive (SRA) (SRR12086708-SRR12086765). All assembled transcriptomes, alignments, inferred gene, and species trees, fossil calibrated phylogenies (including paleontological record assessed from PaleoDB used to plot the fossil distribution in Fig. 1), PhyloNet results, QS results, and introgression results are available on figshare (<https://doi.org/>

10.6084/m9.figshare.12518660). Custom scripts that were used to create various input files as well as the analysis pipeline are available on GitHub [https://github.com/antonysuv/odo\\_introgression](https://github.com/antonysuv/odo_introgression).

#### SUPPLEMENTARY MATERIAL

Data available from the Dryad Digital Repository: <https://doi.org/10.5061/dryad.j3tx95xdp>

#### ACKNOWLEDGMENTS

The authors thank Gavin Martin, Nathan Lord, and Camilla Sharkey for the generation of sequence data. They also thank the DNA Sequencing Center and Fulton Supercomputer Lab (BYU) for assistance. Additionally, they thank Aaron Comeault for his invaluable comments on the manuscript. They are grateful for thoughtful comments and suggestions from the Editors and two anonymous Reviewers that helped improve this manuscript.

#### FUNDING

This work was supported by the National Science Foundation (NSF) grant DEB-1265714 to S.M.B. and the National Institutes of Health (NIH) grants R01HG008696 and R35GM138286 to D.R.S. C.S. was funded by grant ANR-19-CE45-0012 from French Agence Nationale de la Recherche.

#### AUTHOR CONTRIBUTIONS

A.S., C.S., D.R.S., and S.M.B. conceived the research. A.S., C.S., M.S.F., and P.B. analyzed the data. M.C., K.A.C., M.F.W., and D.R.S. supervised the project. A.S., C.S., D.R.S., and S.M.B. wrote the manuscript.

#### REFERENCES

- Aberer A.J., Kobert K., Stamatakis A. 2014. ExaBayes: massively parallel bayesian tree inference for the whole-genome era. *Mol. Biol. Evol.* 31:2553–2556.
- Asahina S., Asahina S., Nihon Gakujutsu S. 1954. A morphological study of a relic dragonfly *Epiophlebia superstes* selys: (Odonata, Anisozygoptera). *Jpn. Soc. Promot. Sci.*
- Barnard A.A., Fincke O.M., McPeck M.A., Masly J.P. 2017. Mechanical and tactile incompatibilities cause reproductive isolation between two young damselfly species. *Evolution* 71:2410–2427.
- Blanke A., Beckmann F., Misof B. 2013. The head anatomy of *Epiophlebia superstes* (Odonata: Epiophlebiidae). *Org. Divers. Evol.* 13:55–66.
- Blanke A., Greve C., Mokso R., Beckmann F., Misof B. 2013. An updated phylogeny of Anisoptera including formal convergence analysis of morphological characters. *Syst. Entomol.* 38:474–490.
- Blischak P.D., Chifman J., Wolfe A.D., Kubatko L.S. 2018. HyDe: a python package for genome-scale hybridization detection. *Syst. Biol.* 67:821–829.
- Bonfante B., Faux P., Navarro N., Mendoza-Revilla J., Dubied M., Montillot C., Wentworth E., Poloni L., Varón-González C., Jones

- P., Xiong Z., Fuentes-Guajardo M., Palma S., Chacón-Duque J.C., Hurtado M., Villegas V., Granja V., Jaramillo C., Arias W., Barquera R., Everardo-Martínez P., Sánchez-Quinto M., Gómez-Valdés J., Villamil-Ramírez H., Cerqueira C.C.S. de Hünemeier T., Ramallo V., Liu F., Weinberg S.M., Shaffer J.R., Stergiakouli E., Howe L.J., Hysi P.G., Spector T.D., Gonzalez-José R., Schöler-Faccini L., Bortolini M.-C., Acuña-Alonzo V., Canizales-Quinteros S., Gallo C., Poletti G., Bedoya G., Rothhammer F., Thauvin-Robinet C., Faivre L., Costedoat C., Balding D., Cox T., Kayser M., Duplomb L., Yalcin B., Cotney J., Adhikari K., Ruiz-Linares A. 2021. A GWAS in Latin Americans identifies novel face shape loci, implicating VPS13B and a Denisovan introgressed region in facial variation. *Sci. Adv.* 7:eabc6160.
- Britton T., Anderson C.L., Jacquet D., Lundqvist S., Bremer K. 2007. Estimating divergence times in large phylogenetic trees. *Syst. Biol.* 56:741–752.
- Brooks S.P., Gelman A. 1998. General methods for monitoring convergence of iterative simulations. *J. Comput. Graphical Stat.* 7:434–455.
- Buchfink B., Xie C., Huson D.H. 2015. Fast and sensitive protein alignment using DIAMOND. *Nat. Methods* 12:59–60.
- Busse S., Genet C., Hornschemeyer T. 2013. Homologization of the flight musculature of zygoptera (insecta: odonata) and neoptera (insecta). *PLoS One* 8:e55787.
- Busse S., Helmker B., Hornschemeyer T. 2015. The thorax morphology of Epiophlebia (Insecta: Odonata) nymphs—including remarks on ontogenesis and evolution. *Sci. Rep.* 5:12835.
- Bybee S., Córdoba-Aguilar A., Duryea M.C., Futahashi R., Hansson B., Lorenzo-Carballea M.O., Schilder R., Stoks R., Suvorov A., Svensson E.I., *et al.* 2016. Odonata (dragonflies and damselflies) as a bridge between ecology and evolutionary genomics. *Front. Zool.* 13:46.
- Bybee S.M., Ogden T.H., Branham M.A., Whiting M.F. 2008. Molecules, morphology and fossils: a comprehensive approach to odonate phylogeny and the evolution of the odonate wing. *Cladistics* 24:477–514.
- Carle F. 2012. A new Epiophlebia (Odonata: Epiophlebioidea) from China with a review of epiophlebian taxonomy, life history, and biogeography. *Arthropod Syst. Phylog.* 70:75–83.
- Carle F.L., Kjer K.M., May M.L. 2008. Evolution of Odonata, with special reference to Coenagrionoidea (Zygoptera). *Arthropod Syst. Phylog.* 66:37–44.
- Carle F.L., Kjer K.M., May M.L. 2015. A molecular phylogeny and classification of Anisoptera (Odonata). *Arthropod Syst. Phylog.* 73:281–301.
- Charles-Elie R., Vincent B., Jean-Christophe G., Fabio P., Scornavacca C. 2020. On the inference of complex phylogenetic networks by Markov Chain Monte-Carlo. *bioRxiv* 2020.2010.2007.329425.
- Chauhan P., Hansson B., Kraaijeveld K., de Knijff P., Svensson E.I., Wellenreuther M. 2014. De novo transcriptome of *Ischnura elegans* provides insights into sensory biology, colour and vision genes. *BMC Genomics* 15:808.
- Cordero Rivera A., Andres J.A., Cordoba-Aguilar A., Utzeri C. 2004. Postmating sexual selection: allopatric evolution of sperm competition mechanisms and genital morphology in calopterygid damselflies (Insecta: Odonata). *Evolution* 58:349–359.
- Cordoba-Aguilar A. 2008. Dragonflies and damselflies: model organisms for ecological and evolutionary research. Oxford; New York: Oxford University Press.
- Degnan J.H., Rosenberg N.A. 2009. Gene tree discordance, phylogenetic inference and the multispecies coalescent. *Trends Ecol. Evol.* 24:332–340.
- Dempewolf H., Baute G., Anderson J., Kilian B., Smith C., Guarino L. 2017. Past and future use of wild relatives in crop breeding. *Crop Sci.* 57:1070–1082.
- Dijkstra K.D., Kalkman V.J., Dow R.A., Stokvis F.R., Van Tol J. 2014. Redefining the damselfly families: a comprehensive molecular phylogeny of Zygoptera (Odonata). *Syst. Entomol.* 39:68–96.
- Dijkstra K.D., Monaghan M.T., Pauls S.U. 2014. Freshwater biodiversity and aquatic insect diversification. *Ann. Rev. Entomol.* 59:143–163.
- Doolittle W.F., Baptiste E. 2007. Pattern pluralism and the Tree of Life hypothesis. *Proc. Natl. Acad. Sci. USA* 104:2043.
- Dos Reis M., Yang Z. 2011. Approximate likelihood calculation on a phylogeny for Bayesian estimation of divergence times. *Mol. Biol. Evol.* 28:2161–2172.
- Dumont H.J., Vierstraete A., Vanfleteren J.R. 2010. A molecular phylogeny of the Odonata (Insecta). *Syst. Entomol.* 35:6–18.
- Durand E.Y., Patterson N., Reich D., Slatkin M. 2011. Testing for ancient admixture between closely related populations. *Mol. Biol. Evol.* 28:2239–2252.
- Eberhard W.G. 2004. Rapid divergent evolution of sexual morphology: comparative tests of antagonistic coevolution and traditional female choice. *Evolution* 58:1947–1970.
- Eckert A.J., Carstens B.C. 2008. Does gene flow destroy phylogenetic signal? The performance of three methods for estimating species phylogenies in the presence of gene flow. *Mol. Phylogenet. Evol.* 49:832–842.
- Eddy S.R. 2011. Accelerated profile HMM searches. *PLoS Comput. Biol.* 7:e1002195.
- Edelman N.B., Frandsen P.B., Miyagi M., Clavijo B., Davey J., Dikow R.B., Garcia-Accinelli G., Van Belleghem S.M., Patterson N., Neafsey D.E., *et al.* 2019. Genomic architecture and introgression shape a butterfly radiation. *Science* 366:594–599.
- Elgvin T.O., Trier C.N., Tørresen O.K., Hagen I.J., Lien S., Nederbragt A.J., Ravinet M., Jensen H., Sætre G.-P. 2017. The genomic mosaicism of hybrid species. *Sci. Adv.* 3:e1602996.
- Figueiro H.V., Li G., Trindade F.J., Assis J., Pais F., Fernandes G., Santos S.H.D., Hughes G.M., Komissarov A., Antunes A., *et al.* 2017. Genome-wide signatures of complex introgression and adaptive evolution in the big cats. *Sci. Adv.* 3:e1700299.
- Fontaine M.C., Pease J.B., Steele A., Waterhouse R.M., Neafsey D.E., Sharakhov I.V., Jiang X., Hall A.B., Catteruccia F., Kakani E., *et al.* 2015. Extensive introgression in a malaria vector species complex revealed by phylogenomics. *Science* 347:1258524.
- Fu L., Niu B., Zhu Z., Wu S., Li W. 2012. CD-HIT: accelerated for clustering the next-generation sequencing data. *Bioinformatics* 28:3150–3152.
- Fujimoto M.S., Suvorov A., Jensen N.O., Clement M.J., Bybee S.M. 2016. Detecting false positive sequence homology: a machine learning approach. *BMC Bioinformatics* 17:101.
- Fujimoto M.S., Suvorov A., Jensen N.O., Clement M.J., Snell Q., Bybee S.M. 2017. The OGCleaner: filtering false-positive homology clusters. *Bioinformatics* 33:125–127.
- Gadagkar S.R., Rosenberg M.S., Kumar S. 2005. Inferring species phylogenies from multiple genes: concatenated sequence tree versus consensus gene tree. *J. Exp. Zool. B Mol. Dev. Evol.* 304:64–74.
- Glémin S., Scornavacca C., Dainat J., Burgarella C., Viader V., Ardisson M., Sarah G., Santoni S., David J., Ranwez V. 2019. Pervasive hybridizations in the history of wheat relatives. *Sci. Adv.* 5:eaav9188.
- Gouy A., Excoffier L. 2020. Polygenic patterns of adaptive introgression in modern humans are mainly shaped by response to pathogens. *Mol. Biol. Evol.* 37:1420–1433.
- Grabherr M.G., Haas B.J., Yassour M., Levin J.Z., Thompson D.A., Amit I., Adiconis X., Fan L., Raychowdhury R., Zeng Q., *et al.* 2011. Full-length transcriptome assembly from RNA-Seq data without a reference genome. *Nat. Biotechnol.* 29:644–652.
- Green R.E., Krause J., Briggs A.W., Maricic T., Stenzel U., Kircher M., Patterson N., Li H., Zhai W., Fritz M.H., *et al.* 2010. A draft sequence of the Neandertal genome. *Science* 328:710–722.
- Grimaldi D.A., Engel M.S. 2005. Evolution of the insects. Cambridge (UK); New York (NY): Cambridge University Press.
- Guerrero R.F., Hahn M.W. 2018. Quantifying the risk of hemiplasy in phylogenetic inference. *Proc. Natl. Acad. Sci. USA* 115:12787–12792.
- Haas B.J., Papanicolaou A., Yassour M., Grabherr M., Blood P.D., Bowden J., Couger M.B., Eccles D., Li B., Lieber M., *et al.* 2013. De novo transcript sequence reconstruction from RNA-seq using the Trinity platform for reference generation and analysis. *Nat. Protoc.* 8:1494–1512.
- Hahn M.W., Hibbins M.S. 2019. A three-sample test for introgression. *Mol. Biol. Evol.* 36:2878–2882.
- Hallstrom B.M., Janke A. 2010. Mammalian evolution may not be strictly bifurcating. *Mol. Biol. Evol.* 27:2804–2816.
- Harrison R.G., Larson E.L. 2014. Hybridization, introgression, and the nature of species boundaries. *J. Heredity* 105:795–809.
- Hasegawa E., Kasuya E. 2006. Phylogenetic analysis of the insect order Odonata using 28S and 16S rDNA sequences: a comparison between data sets with different evolutionary rates. *Entomol. Sci.* 9:55–66.

- Hayashi F., Dobata S., Futahashi R. 2005. Disturbed population genetics: suspected introgressive hybridization between two Mnais damselfly species (Odonata). *Zool. Sci.* 22:869–881.
- Heled J., Drummond A.J. 2010. Bayesian inference of species trees from multilocus data. *Mol. Biol. Evol.* 27:570–580.
- Heliconius Genome Consortium. 2012. Butterfly genome reveals promiscuous exchange of mimicry adaptations among species. *Nature* 487:94–98.
- Hellmuth M., Wieseke N., Lechner M., Lenhof H.P., Middendorf M., Stadler P.F. 2015. Phylogenomics with paralogs. *Proc. Natl. Acad. Sci. USA* 112:2058–2063.
- Hermansen J.S., Sæther S.A., Elgvin T.O., Borge T., Hjelle E., Sætre G-P. 2011. Hybrid speciation in sparrows I: phenotypic intermediacy, genetic admixture and barriers to gene flow. *Mol. Ecol.* 20:3812–3822.
- Hibbins M., Hahn M., 2021. Phylogenomic approaches to detecting and characterizing introgression. *EcoEvoRxiv* doi: 10.32942/osf.io/uahd8.
- Hosken D.J., Stockley P. 2004. Sexual selection and genital evolution. *Trends Ecol. Evol.* 19:87–93.
- Huerta-Sanchez E., Jin X., Asan, Bianba Z., Peter B.M., Vinckenbosch N., Liang Y., Yi X., He M., Somel M., *et al.* 2014. Altitude adaptation in Tibetans caused by introgression of Denisovan-like DNA. *Nature* 512:194–197.
- Huson D.H., Klöpper T., Lockhart P.J., Steel M.A. 2005. Reconstruction of reticulate networks from gene trees. In: Miyano S., Mesirov J., Kasif S., Istrail S., Pevzner P.A., Waterman M., editors. *Research in computational molecular biology*. Berlin (Heidelberg): Springer Berlin Heidelberg. p. 233–249.
- Janzen G.M., Wang L., Hufford M.B. 2019. The extent of adaptive wild introgression in crops. *New Phytol.* 221:1279–1288.
- Jones G.R. 2019. Divergence estimation in the presence of incomplete lineage sorting and migration. *Syst. Biol.* 68:19–31.
- Káldy J., Mozsár A., Fazekas G., Farkas M., Fazekas D.L., Fazekas G.L., Goda K., Gyöngy Z., Kovács B., Semmens K., Bercsényi M., Molnár M., Patakiné Várkonyi E. 2020. Hybridization of Russian Sturgeon (*Acipenser gueldenstaedtii*, Brandt and Ratzeberg, 1833) and American Paddlefish (*Polyodon spathula*, Walbaum 1792) and evaluation of their progeny. *Genes (Basel)* 11:753.
- Kim M.J., Jung K.S., Park N.S., Wan X., Kim K.-G., Jun J., Yoon T.J., Bae Y.J., Lee S.M., Kim I. 2014. Molecular phylogeny of the higher taxa of Odonata (Insecta) inferred from COI, 16S rRNA, 28S rRNA, and EF1- $\alpha$  sequences. *Entomol. Res.* 44:65–79.
- Kong S., Kubatko L.S. 2021. Comparative performance of popular methods for hybrid detection using genomic data. *Syst. Biol.* 70:891–907.
- Kubatko L.S., Chifman J. 2019. An invariants-based method for efficient identification of hybrid species from large-scale genomic data. *BMC Evol. Biol.* 19:112.
- Kubatko L.S., Degnan J.H. 2007. Inconsistency of phylogenetic estimates from concatenated data under coalescence. *Syst. Biol.* 56:17–24.
- Kunte K., Shea C., Aardema M.L., Scriber J.M., Juenger T.E., Gilbert L.E., Kronforst M.R. 2011. Sex chromosome mosaicism and hybrid speciation among tiger swallowtail butterflies. *PLoS Genet.* 7:e1002274.
- Kuznetsova V.G., Golub N.V. 2020. A checklist of chromosome numbers and a review of karyotype variation in Odonata of the world. *Comp. Cytogenet.* 14:501–540.
- Labandeira C.C., Sepkoski J.J. Jr. 1993. Insect diversity in the fossil record. *Science* 261:310–315.
- Lai Z., Nakazato T., Salmaso M., Burke J.M., Tang S., Knapp S.J., Rieseberg L.H. 2005. Extensive chromosomal repatterning and the evolution of sterility barriers in hybrid sunflower species. *Genetics* 171:291–303.
- Lakner C., van der Mark P., Huelsenbeck J.P., Larget B., Ronquist F. 2008. Efficiency of Markov chain Monte Carlo tree proposals in Bayesian phylogenetics. *Syst. Biol.* 57:86–103.
- Landry C.R., Wittkopp P.J., Taubes C.H., Ranz J.M., Clark A.G., Hartl D.L. 2005. Compensatory cis-trans evolution and the dysregulation of gene expression in interspecific hybrids of *Drosophila*. *Genetics* 171:1813–1822.
- Lanfear R., Calcott B., Kainer D., Mayer C., Stamatakis A. 2014. Selecting optimal partitioning schemes for phylogenomic datasets. *BMC Evol. Biol.* 14:82.
- Lanfear R., Frandsen P.B., Wright A.M., Senfeld T., Calcott B. 2017. PartitionFinder 2: new methods for selecting partitioned models of evolution for molecular and morphological phylogenetic analyses. *Mol. Biol. Evol.* 34:772–773.
- Lanfear R., Hua X., Warren D.L. 2017. Estimating the effective sample size of tree topologies from Bayesian phylogenetic analyses. *Genome Biol. Evol.* 8:2319–2332.
- Leaché A.D., Harris R.B., Rannala B., Yang Z. 2014. The influence of gene flow on species tree estimation: a simulation study. *Syst. Biol.* 63:17–30.
- Lemmon E.M., Lemmon A.R. 2010. Reinforcement in chorus frogs: lifetime fitness estimates including intrinsic natural selection and sexual selection against hybrids. *Evolution* 64:1748–1761.
- Letsch H., Gottsberger B., Ware J.L. 2016. Not going with the flow: a comprehensive time-calibrated phylogeny of dragonflies (Anisoptera: Odonata: Insecta) provides evidence for the role of lentic habitats on diversification. *Mol. Ecol.* 25:1340–1353.
- Li G., Davis B.W., Eizirik E., Murphy W.J. 2016. Phylogenomic evidence for ancient hybridization in the genomes of living cats (Felidae). *Genome Res.* 26:1–11.
- Li L., Stoeckert C.J. Jr., Roos D.S. 2003. OrthoMCL: identification of ortholog groups for eukaryotic genomes. *Genome Res.* 13:2178–2189.
- Liu J., Yu L., Arnold M.L., Wu C.H., Wu S.F., Lu X., Zhang Y.P. 2011. Reticulate evolution: frequent introgressive hybridization among Chinese hares (genus *Lepus*) revealed by analyses of multiple mitochondrial and nuclear DNA loci. *BMC Evol. Biol.* 11:223.
- Lowe C., Harvey I., Thompson D., Watts P. 2008. Strong genetic divergence indicates that congeneric damselflies *Coenagrion puella* and *C. pulchellum* (Odonata: Zygoptera: Coenagrionidae) do not hybridize. *Hydrobiologia* 605:55–63.
- Loytynoja A. 2014. Phylogeny-aware alignment with PRANK. *Methods Mol. Biol.* 1079:155–170.
- Loytynoja A., Goldman N. 2008. Phylogeny-aware gap placement prevents errors in sequence alignment and evolutionary analysis. *Science* 320:1632–1635.
- Maddison W.P. 1997. Gene trees in species trees. *Syst. Biol.* 46:523–536.
- Mallet J. 2005. Hybridization as an invasion of the genome. *Trends Ecol. Evol.* 20:229–237.
- Mallet J., Besansky N., Hahn M.W. 2016. How reticulated are species? *Bioessays* 38:140–149.
- Martin S.H., Davey J.W., Jiggins C.D. 2015. Evaluating the use of ABBA-BABA statistics to locate introgressed loci. *Mol. Biol. Evol.* 32:244–257.
- Martin S.H., Jiggins C.D. 2017. Interpreting the genomic landscape of introgression. *Curr. Opin. Genet. Dev.* 47:69–74.
- Matushkina N.A. 2008. The ovipositor of the relic dragonfly *Epiophlebia superstes*: a morphological re-examination (Odonata: Epiophlebiidae). *Int. J. Odonatol.* 11:71–80.
- McVay J.D., Hipp A.L., Manos P.S. 2017. A genetic legacy of introgression confounds phylogeny and biogeography in oaks. *Proc. R. Soc. B Biol. Sci.* 284:20170300.
- Meier J.I., Marques D.A., Mwaiko S., Wagner C.E., Excoffier L., Seehausen O. 2017. Ancient hybridization fuels rapid cichlid fish adaptive radiations. *Nat. Commun.* 8:14363.
- Mendes F.K., Hahn M.W. 2016. Gene tree discordance causes apparent substitution rate variation. *Syst. Biol.* 65:711–721.
- Meng C., Kubatko L.S. 2009. Detecting hybrid speciation in the presence of incomplete lineage sorting using gene tree incongruence: a model. *Theor. Popul. Biol.* 75:35–45.
- Minh B.Q., Nguyen M.A., von Haeseler A. 2013. Ultrafast approximation for phylogenetic bootstrap. *Mol. Biol. Evol.* 30:1188–1195.
- Mirarab S., Nguyen N., Guo S., Wang L.S., Kim J., Warnow T. 2015. PASTA: ultra-large multiple sequence alignment for nucleotide and amino-acid sequences. *J. Comput. Biol.* 22:377–386.
- Mirarab S., Reaz R., Bayzid M.S., Zimmermann T., Swenson M.S., Warnow T. 2014. ASTRAL: genome-scale coalescent-based species tree estimation. *Bioinformatics* 30:i541–i548.
- Misof B., Liu S., Meusemann K., Peters R.S., Donath A., Mayer C., Frandsen P.B., Ware J., Flouri T., Beutel R.G., *et al.* 2014. Phylogenomics resolves the timing and pattern of insect evolution. *Science* 346:763–767.

- Misof B., Misof K. 2009. A Monte Carlo approach successfully identifies randomness in multiple sequence alignments: a more objective means of data exclusion. *Syst. Biol.* 58:21–34.
- Misof B., Rickert A.M., Buckley T.R., Fleck G., Sauer K.P. 2001. Phylogenetic signal and its decay in mitochondrial SSU and LSU rRNA gene fragments of Anisoptera. *Mol. Biol. Evol.* 18: 27–37.
- Monetti L., Sánchez-Guillén R.A., Rivera A.C. 2002. Hybridization between *Ischnura graellsii* (Vander Linder) and *I. elegans* (Rambur) (Odonata: Coenagrionidae): are they different species? *Biol. J. Linn. Soc.* 76:225–235.
- Nel A., Bechly G., Martínez-Delclos X., Fleck G. 2001. A new family of Anisoptera from the Upper Jurassic of Karatau in Kazakhstan (Insecta: Odonata: Juragomphidae n. fam.). *Stuttgart. Beitr. Naturkd. B (Geol. Palaeontol.)*, 314:1–9.
- Nguyen L.T., Schmidt H.A., von Haeseler A., Minh B.Q. 2015. IQ-TREE: a fast and effective stochastic algorithm for estimating maximum-likelihood phylogenies. *Mol. Biol. Evol.* 32:268–274.
- Nolte A.W., Tautz D. 2010. Understanding the onset of hybrid speciation. *Trends Genet.* 26:54–58.
- Norris L.C., Main B.J., Lee Y., Collier T.C., Fofana A., Cornel A.J., Lanzaro G.C. 2015. Adaptive introgression in an African malaria mosquito coincident with the increased usage of insecticide-treated bed nets. *Proc. Natl. Acad. Sci. USA* 112:815–820.
- Ogden T.H., Whiting M.F. 2003. The problem with “the Paleoptera Problem:” sense and sensitivity. *Cladistics* 19:432–442.
- Ogilvie H.A., Bouckaert R.R., Drummond A.J. 2017. StarBEAST2 brings faster species tree inference and accurate estimates of substitution rates. *Mol. Biol. Evol.* 34:2101–2114.
- Ogilvie H.A., Heled J., Xie D., Drummond A.J. 2016. Computational performance and statistical accuracy of \*BEAST and comparisons with other methods. *Syst. Biol.* 65:381–396.
- Oziolor E.M., Reid N.M., Yair S., Lee K.M., Guberman Verploeg S., Bruns P.C., Shaw J.R., Whitehead A., Matson C.W. 2019. Adaptive introgression enables evolutionary rescue from extreme environmental pollution. *Science* 364:455–457.
- Patterson N., Moorjani P., Luo Y., Mallick S., Rohland N., Zhan Y., Genschoreck T., Webster T., Reich D. 2012. Ancient admixture in human history. *Genetics* 192:1065–1093.
- Pease J.B., Brown J.W., Walker J.F., Hinchliff C.E., Smith S.A. 2018. Quartet sampling distinguishes lack of support from conflicting support in the green plant tree of life. *Am. J. Bot.* 105:385–403.
- Pease J.B., Hahn M.W. 2015. Detection and polarization of introgression in a five-taxon phylogeny. *Syst. Biol.* 64:651–662.
- Perry W.L., Lodge D.M., Feder J.L. 2002. Importance of hybridization between indigenous and nonindigenous freshwater species: an overlooked threat to North American biodiversity. *Syst. Biol.* 51:255–275.
- Petr M., Paabo S., Kelso J., Vernet B. 2019. Limits of long-term selection against Neandertal introgression. *Proc. Natl. Acad. Sci. USA* 116:1639–1644.
- Pfau H.K. 1991. Contributions of functional morphology to the phylogenetic systematics of Odonata. *Adv. Odonatol.* 5:109–141.
- Posada D., Crandall K.A. 2001. Intraspecific gene genealogies: trees grafting into networks. *Trends Ecol. Evol.* 16:37–45.
- Puttick M.N. 2019. MCMCTreeR: functions to prepare MCMCtree analyses and visualize posterior ages on trees. *Bioinformatics* 35:5321–5322.
- Quilodrán C.S., Montoya-Burgos J.I., Currat M. 2020. Harmonizing hybridization dissonance in conservation. *Commun. Biol.* 3:391.
- Rambaut A., Drummond A.J., Xie D., Baele G., Suchard M.A. 2018. Posterior summarization in Bayesian phylogenetics using tracer 1.7. *Syst. Biol.* 67:901–904.
- Rehn A.C. 2003. Phylogenetic analysis of higher-level relationships of Odonata. *Syst. Entomol.* 28:181–240.
- Roch S., Steel M. 2014. Likelihood-based tree reconstruction on a concatenation of aligned sequence data sets can be statistically inconsistent. *Theor. Popul. Biol.* 100C:56–62.
- Rohde R.A., Muller R.A. 2005. Cycles in fossil diversity. *Nature* 434:208–210.
- Rothfels C.J., Johnson A.K., Hovenkamp P.H., Swofford D.L., Roskam H.C., Fraser-Jenkins C.R., Windham M.D., Pryer K.M. 2015. Natural hybridization between genera that diverged from each other approximately 60 million years ago. *Am. Nat.* 185:433–442.
- Runemark A., Vallejo-Marin M., Meier J.I. 2019. Eukaryote hybrid genomes. *PLoS Genet.* 15:e1008404.
- Ruppell G., Hilfert D. 1993. The flight of the relict dragonfly *Epiophlebia superstes* in comparison with that of the modern Odonata. *Odonatologica* 22:295–309.
- Sánchez-Guillén R.A., Córdoba-Aguilar A., Cordero-Rivera A., Wellenreuther M. 2014. Genetic divergence predicts reproductive isolation in damselflies. *J. Evol. Biol.* 27:76–87.
- Sánchez-Guillén R.A., Van Gossum H., Cordero Rivera A. 2005. Hybridization and the inheritance of female colour polymorphism in two ischnurid damselflies (Odonata: Coenagrionidae). *Biol. J. Linn. Soc.* 85:471–481.
- Sánchez-Guillén R.A., Wellenreuther M., Cordero-Rivera A., Hansson B. 2011. Introgression and rapid species turnover in sympatric damselflies. *BMC Evol. Biol.* 11:210.
- Saux C., Simon C., Spicer G.S. 2003. Phylogeny of the dragonfly and damselfly order Odonata as inferred by mitochondrial 12S ribosomal RNA sequences. *Ann. Entomol. Soc. Am.* 96:693–699.
- Sayyari E., Mirarab S. 2016. Fast coalescent-based computation of local branch support from quartet frequencies. *Mol. Biol. Evol.* 33:1654–1668.
- Schumer M., Rosenthal G.G., Andolfatto P. 2014. How common is homoploid hybrid speciation? *Evolution* 68:1553–1560.
- Seehausen O. 2004. Hybridization and adaptive radiation. *Trends Ecol. Evol.* 19:198–207.
- Simao F.A., Waterhouse R.M., Ioannidis P., Kriventseva E.V., Zdobnov E.M. 2015. BUSCO: assessing genome assembly and annotation completeness with single-copy orthologs. *Bioinformatics* 31:3210–3212.
- Solano E., Hardersen S., Audisio P., Amorosi V., Senczuk G., Antonini G. 2018. Asymmetric hybridization in Cordulegaster (Odonata: Cordulegasteridae): secondary postglacial contact and the possible role of mechanical constraints. *Ecol. Evol.* 8:9657–9671.
- Solis-Lemus C., Yang M., Ané C. 2016. Inconsistency of species tree methods under gene flow. *Syst. Biol.* 65:843–851.
- Suvorov A., Jensen N.O., Sharkey C.R., Fujimoto M.S., Bodily P., Wightman H.M., Ogden T.H., Clement M.J., Bybee S.M. 2017. Opsins have evolved under the permanent heterozygote model: insights from phylotranscriptomics of Odonata. *Mol. Ecol.* 26:1306–1322.
- Suvorov A., Kim B.Y., Wang J., Armstrong E.E., Peede D., D’Agostino E.R.R., Price D.K., Wadell P., Lang M., Courtier-Ordogozo V., et al. 2021. Widespread introgression across a phylogeny of 155 “Drosophila” genomes. *bioRxiv*: 2020.2012.2014.422758.
- Svardal H., Quah F.X., Malinsky M., Ngatunga B.P., Miska E.A., Salzburger W., Genner M.J., Turner G.F., Durbin R. 2020. Ancestral hybridization facilitated species diversification in the Lake Malawi Cichlid fish adaptive radiation. *Mol. Biol. Evol.* 37:1100–1113.
- Tennesen K. 1982. Review of reproductive isolating barriers in Odonata. *Adv. Odonatol.* 1:251–265.
- Than C., Ruths D., Nakhleh L. 2008. PhyloNet: a software package for analyzing and reconstructing reticulate evolutionary relationships. *BMC Bioinformatics* 9:322.
- Thomas J.A., Trueman J.W., Rambaut A., Welch J.J. 2013. Relaxed phylogenetics and the palaeoptera problem: resolving deep ancestral splits in the insect phylogeny. *Syst. Biol.* 62:285–297.
- Troast D., Suhling F., Jinguji H., Sahlen G., Ware J. 2016. A global population genetic study of *Pantala flavescens*. *PLoS One*, 11:e0148949.
- Trueman J.W.H. 1996. A preliminary cladistic analysis of odonate wing venation. *Odonatologica* 25:59–72.
- Tynkynen K., Grapputo A., Kotiaho J.S., Rantala M.J., Väänänen S., Suhonen J. 2008. Hybridization in *Calopteryx damselflies*: the role of males. *Anim. Behav.* 75:1431–1439.
- van der Maaten L., Hinton G. 2008. Visualizing data using t-SNE. *J. Mach. Learn. Res.* 9:2579–2605.
- Vanderpool D., Minh B.Q., Lanfear R., Hughes D., Murali S., Harris R.A., Raveendran M., Muzny D.M., Hibbins M.S., Williamson R.J., et al. 2020. Primate phylogenomics uncovers multiple rapid radiations and ancient interspecific introgression. *PLoS Biol.* 18:e3000954.
- vonHoldt B.M., Pollinger J.P., Earl D.A., Knowles J.C., Boyko A.R., Parker H., Geffen E., Pilot M., Jedrzejewski W., Jedrzejewska B., et al. 2011. A genome-wide perspective on the evolutionary history of

- enigmatic wolf-like canids. *Genome Res.* 21:1294–1305.
- Wang M., Zhao Y., Zhang B. 2015. Efficient test and visualization of multi-set intersections. *Sci. Rep.* 5:16923.
- Wang X., He Z., Shi S., Wu C.-I. 2020. Genes and speciation: is it time to abandon the biological species concept? *Natl. Sci. Rev.* 7:1387–1397.
- Wang Y., Cao Z., Ogilvie H.A., Nakhleh L. 2020. Phylogenomic assessment of the role of hybridization and introgression in trait evolution. *bioRxiv*: 2020.2009.2016.300343.
- Ware J., May M., Kjer K. 2007. Phylogeny of the higher Libelluloidea (Anisoptera: Odonata): an exploration of the most speciose superfamily of dragonflies. *Mol. Phylogenet. Evol.* 45:289–310.
- Wen D., Yu Y., Zhu J., Nakhleh L. 2018. Inferring phylogenetic networks using PhyloNet. *Syst. Biol.* 67:735–740.
- Wickett N.J., Mirarab S., Nguyen N., Warnow T., Carpenter E., Matasci N., Ayyampalayam S., Barker M.S., Burleigh J.G., Gitzendanner M.A., *et al.* 2014. Phylotranscriptomic analysis of the origin and early diversification of land plants. *Proc. Natl. Acad. Sci. USA* 111:E4859–E4868.
- Yang Y., Smith S.A. 2014. Orthology inference in nonmodel organisms using transcriptomes and low-coverage genomes: improving accuracy and matrix occupancy for phylogenomics. *Mol. Biol. Evol.* 31:3081–3092.
- Yang Z. 2007. PAML 4: phylogenetic analysis by maximum likelihood. *Mol. Biol. Evol.* 24:1586–1591.
- Yi H., Jin L. 2013. Co-phylog: an assembly-free phylogenomic approach for closely related organisms. *Nucleic Acids Res.* 41:e75.
- Yu Y., Nakhleh L. 2015. A maximum pseudo-likelihood approach for phylogenetic networks. *BMC Genomics* 16:S10.
- Yu Y., Than C., Degnan J.H., Nakhleh L. 2011. Coalescent histories on phylogenetic networks and detection of hybridization despite incomplete lineage sorting. *Syst. Biol.* 60:138–149.
- Zhang D, Rheindt F.E., She H., Cheng Y., Song G., Jia C., Qu Y., Alström P., Lei F. 2021. Most genomic loci misrepresent the phylogeny of an avian radiation because of ancient gene flow. *Syst. Biol.* 70: 961–975.